

Rigaku VariMax Dual

Part 2a Analysis Manual with CrystalStructure 4.2

X-ray Laboratory, Nano-Engineering Research Center, Institute of Engineering Innovation, The University of Tokyo

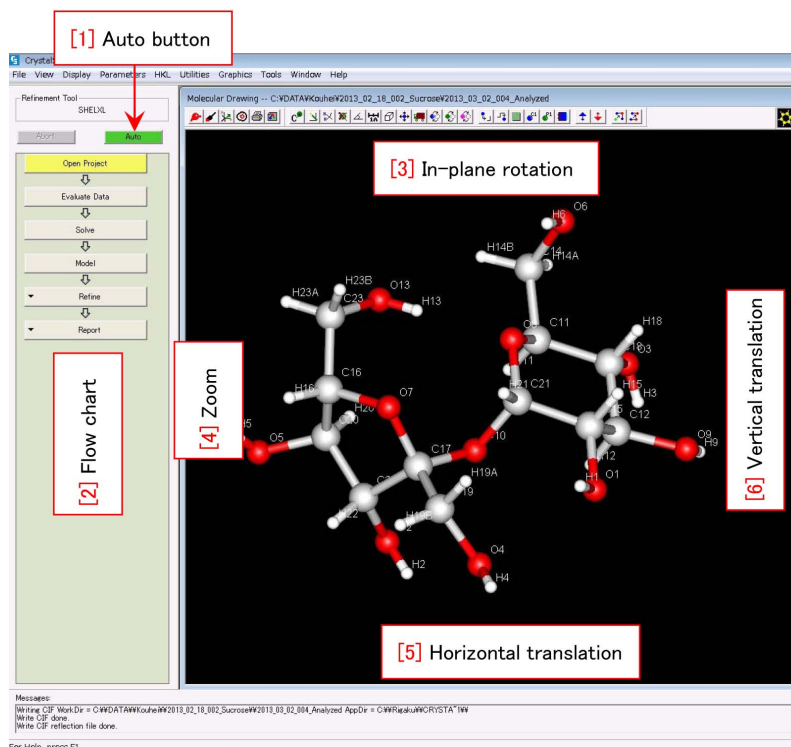


Figure 0: Whole window of CrystalStructure. Molecular structure of sucrose.

Molecular structure of sucrose has been solved from diffraction data measured with CryAlis^{Pro}. At first, '*.cif.od' should be opened by clicking 'Open Project' in '[2] Flow chart'. The above structure has been obtained only by clicking '[1] Auto' button. This is a fortunate case for a high-quality crystal of molecule with relatively simple structure.

The procedures shown in '[2] Flow chart' should usually be done from up to down. The molecular model can be three-dimensionally rotated by click&dragging the central part of the window. Places around which indicated by '[3] In-plane rotation', '[4] Zoom', '[5] Horizontal translation' and '[6] Vertical translation' can be click&dragged to do these operations.

'CrystalStructure 4.1' can be used also on a Dell computer that is placed near the entrance of the room, other than the control computer for VariMax Dual in the same room (333). Dell computer can be logged in by typing 'hprray' both for user name and password.

In Appendix A [p.20], how reasonably defined the reciprocal lattice is, is described

In Appendix B [p.24], how to determine the space group from consideration on extinction rules.

In Appendix C [p.37], the reason for representing reflection vectors with four indices and extinction rules for trigonal and hexagonal crystal systems.

Mathematical proofs for extinction rules described in Appendices B [p.24] and C [p.37] are recommended to read for further understanding of extinction rules when the reader has time.

Contents

1	Making an account	1
1.1	Making an account	1
2	Determination of molecular structure with ‘CrystalStructure’	3
2.1	Open Project	3
2.2	Change of the parameters	4
2.2.1	Setting of the X-rays	4
2.2.2	Setting the diffractometer and the detector	4
2.2.3	Change of the value of Z	5
2.3	Selection of the refinement tools	5
2.4	Preprocessing measured data	6
2.4.1	Averaging equivalent diffraction data	6
2.5	Phase determination and calculation of molecular model	7
2.5.1	Direct method	7
2.5.2	Phase problem in cases of centrosymmetric crystals	7
2.5.3	Determination of initial phases with the direct method	7
2.6	Optimization of the molecular structure	9
2.6.1	Optimization with isotropic temperature factors	9
2.6.2	Optimization with anisotropic temperature factors	9
2.7	Optimization taking into account hydrogen atoms	11
2.7.1	Automatic assignment of hydrogen atoms	11
2.7.2	Manual assignment of hydrogen atoms	11
2.7.3	Execution of least square fitting	12
2.8	Making a report	15
2.8.1	Making an rtf file	15
2.8.2	Making CIF files	16
2.9	Loading a CIF file and drawing a molecular model	16
2.9.1	Check of CIF file	16
2.9.2	Drawing the molecular model	17
A	Why should we define ‘Reciprocal Lattice’ ?	20
A.1	Bragg’s reflection condition	20
A.2	Laue’s reflection condition	20
A.3	Ewald’s reflection condition (Ewald construction)	21
A.3.1	Foundation of Ewald construction	21
A.3.2	Relation between reciprocal lattice vector and Bragg reflection plane	22
A.4	Drawing of Miller and Miller indices	23

B	Determination of space group from extinction rule	24
B.1	Symmetric elements of crystal derived based on the group theory	26
B.2	Symbols of space groups	27
B.3	How to read extinction rules	28
B.4	Examples of extinction rules due to combinations of symmetric elements	29
B.4.1	Orthorhombic $P2_12_12_1$ (#19)	30
B.4.2	Monoclinic $P12_11[P2_1$ (#4)]	30
B.5	Mathematical proofs of extinction rules	31
B.5.1	Extinction rules due to complex lattice	31
B.5.1.1	Extinction due to base-centered lattice	31
B.5.1.2	Extinction due to body-centered lattice	32
B.5.1.3	Extinction due to face-centered lattice	32
B.5.2	Extinction owing to glide axes	33
B.5.2.1	Extinction due to axial glide plane	33
B.5.2.2	Extinction due to double glide plane (e glide plane)	33
B.5.2.3	Extinction due to diagonal glide plane	34
B.5.3	Extinction due to screw axes	34
B.5.3.1	Extinction due to 2_1 screw axis	34
B.5.3.2	Extinction due to 4_1 screw axis	35
B.5.3.3	Extinction due to 4_2 screw axis	35
C	Reflection indices and extinction rules in the cases of trigonal and hexagonal crystals	37
C.1	Cases of trigonal system	37
C.1.1	Diagram shown in <i>International Tables for Crystallography</i> (2006) Vol.A	37
C.1.2	Real and reciprocal coordinates	38
C.1.3	Derivation of extinction rule due to 3_1 screw axis	38
C.1.4	On the absence of extinction due to 2_1 screw axis perpendicular to \mathbf{c}	39
C.2	Case of hexagonal system	40
C.2.1	Figure shown in <i>International Tables for Crystallography</i> (2006) Vol.A	40
C.2.2	Coordinates for describing six-fold screw axes	40
C.2.3	Derivation of extinction rule due to 6_1 screw axis	41
C.2.4	Derivation of the extinction due to 6_2 screw axis	42
C.2.5	Derivation of extinction rule due to 6_3 screw axis	42

List of Figures

0	Whole window of CrystalStructure. Molecular structure of sucrose.	i
1.1	Login window.	1
1.2	'Administration' should be selected from 'Tools' menu.	1
1.3	AdministrationCGeneral tab.	1
1.4	Administration, Users tab.	1
1.5	AdministrationCGroups tab.	2
1.6	AdministrationCServers tab.	2
2.1	Login window.	3
2.2	Project open	3
2.3	Text shown after opening the project	3
2.4	X-ray setting menu	4
2.5	X-ray setting should be changed	4
2.6	Set of the diffractometer	4
2.7	Set of the diffractometer and detector	4
2.8	Set of the molecular formula	4
2.9	Setting the molecular formula and Z value	5
2.10	Selection of refinement tools.	5
2.11	Verification message for changing refinement tools.	5
2.12	Message for average and absorption correction.	6
2.13	Verification message for averaging equivalent diffraction intensities. This message window has been abolished.	6
2.14	Option window for averaging reflections.	6
2.15	Selection of algorithm for phase determination with the direct method.	7
2.16	Success message of phase determination.	8
2.17	Molecular model of solved structure.	8
2.18	Least square fitting window (Shelx).	8
2.19	Least square fitting window (Crystals).	8
2.20	Situation of least-square fitting.	8
2.21	Text window showing fitness of the least square fitting.	9
2.22	Green spheres can be hidden by clicking '[1] Peak ON/OFF' button.	10
2.23	'Refinement attributes' should be clicked.	10
2.24	Position refinement and anisotropic temperature factor are applied for non-hydrogen atoms.	10
2.25	Anisotropic temperature factors have been applied for non-hydrogen atoms.	10
2.26	Shapes of non-hydrogen atoms changed to be cubes.	11
2.27	Window showing the fitting situation.	11
2.28	Process of fitting with hydrogen atoms.	11
2.29	Selection of atoms with no hydrogen.	11
2.30	Selection of hydroxi oxigens.	12

2.31	Selection of methine carbon.	12
2.32	Selection of methylene carbon.	12
2.33	All hydrogen atoms have been assigned.	12
2.34	Refinement settings.	12
2.35	Refinement settings for hydrogen positions.	12
2.36	Refinement settings with ‘Sheldrick’ weights.	13
2.37	Calculation of weights.	13
2.38	Refinement results.	13
2.39	Calculation of weights (again).	14
2.40	Refinement settings (again).	14
2.41	Refinement results (again).	14
2.42	Checking window for publication in Acta Cryst. C (#1).	14
2.43	Checking window for publication in Acta Cryst. C (#2).	14
2.44	Inversion of absolute structure.	15
2.45	Checking window for publication in Acta Cryst. C (#3).	15
2.46	Checking window for publication in Acta Cryst. C (#4; final).	15
2.47	‘Report’ button has been clicked.	15
2.48	Making crystal information file.	15
2.49	Crystal information (*.rtf) file).	16
2.50	Making ‘Cif.Cif’.	16
2.51	‘Open a Browser’ button should be clicked.	16
2.52	Start window of ‘PLATON’.	16
2.53	‘Cif.cif’ should be selected.	16
2.54	‘Cif.cif’ is sent to IUCr web site by clicking ‘Send CIF for checking’ button.	17
2.55	‘PLATON’ for checking the molecular structure has been opened.	17
2.56	Alerts on solved molecular structure.	17
2.57	Thermal ellipsoid model of molecular structure.	17
2.58	Loading ‘Cif.Cif’.	17
2.59	Thermal ellipsoid model of molecular structure.	18
2.60	Thermal ellipsoid model of molecular structure.	18
A.1	Bragg’s reflection condition.	20
A.2	Laue’s reflection condition.	21
A.3	Ewald sphere	22
A.4	Drawing of Miller and Miller indices	23
B.1	Content of ‘process.out’ (#1). [Taurine; monoclinic $P2_1/c$ (#14)].	24
B.2	Content of ‘process.out’ (#2). [Taurine; monoclinic $P2_1/c$ (#14)]	24
B.3	Content of ‘process.out’ (#3) [Taurine; monoclinic $P2_1/c$ (#14)]. [setting #1] corresponds to ‘[1] CELL CHOICE 1’ in Fig. B.5.	25
B.4	Reflection condition of $P2_1/c$ (#14) described in <i>International Tables for Crystallography</i> (2006) Vol.A. $0k0$ reflections when k is odd and, $h0l$ and $00l$ reflections when l is odd, extinguish.	25
B.5	Drawings for space group $P2_1/c$ (#14) in <i>International Tables for Crystallography</i> (2006) Vol.A. Protein crystals do not belong to this space group absolutely.	27
B.6	Redesignation of space group in CrystalStructure 4.1. (in the case of small molecular-weight crystal).	29
B.7	Drawing for $P\bar{1}$ (#2) in <i>International Tables for Crystallography</i> (2006) Vol.A. Since this space group has symmetric center, protein crystals do not belong to it. The phase problem is simple (0 or π (180°)).	29

B.8	Drawing for $C12/c1[C2/c](\#15)$ in <i>International Tables for Crystallography</i> (2006) Vol.A. Protein crystals do not belong to this space group absolutely since it has glide plane.	29
B.9	<i>International Tables for Crystallography</i> (2006) Vol.A $P2_12_12_1(\#19)$	30
B.10	<i>International Tables for Crystallography</i> (2006) Vol.A $P12_11[P2_1(\#4)]$	30
C.1	<i>International Tables for Crystallography</i> (2006) Vol.A, Symmetric elements. $P3_121(\#152)$	37
C.2	<i>International Tables for Crystallography</i> (2006) Vol.A, Positions of atoms. $P3_121(\#152)$	37
C.3	Real (black) and reciprocal (gray) primitive translation vectors.	38
C.4	<i>International Tables for Crystallography</i> (2006) Vol.A, Symmetric elements. $P6_122(\#178)$	40
C.5	<i>International Tables for Crystallography</i> (2006) Vol.A, Positions of atoms. $P6_122(\#178)$	40

Chapter 1

Making an account

If the user already has an account to login the 'CrystalStructure 4.1', the present chapter does not have to be referred. Go to the next chapter 2 [p.3], please.

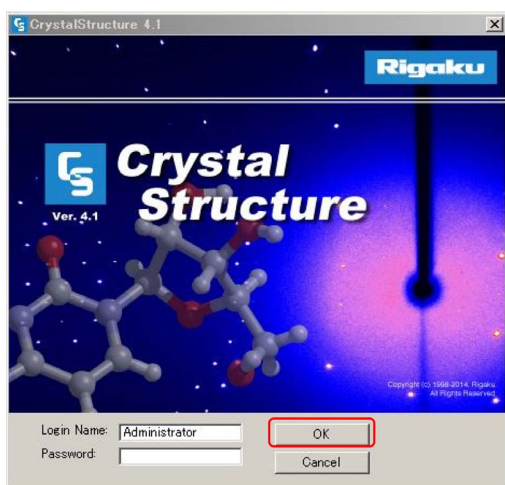


Figure 1.1: Login window.

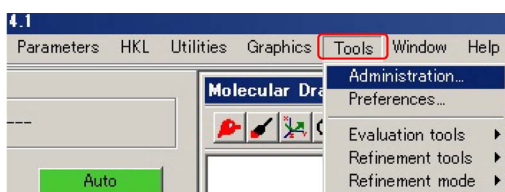


Figure 1.2: 'Administration' should be selected from 'Tools' menu.

1.1 Making an account

Click the icon of 'CrystalStructure 4.1' on the desktop to display Fig. 1.1, please. To make an account for the first time, 'OK' button

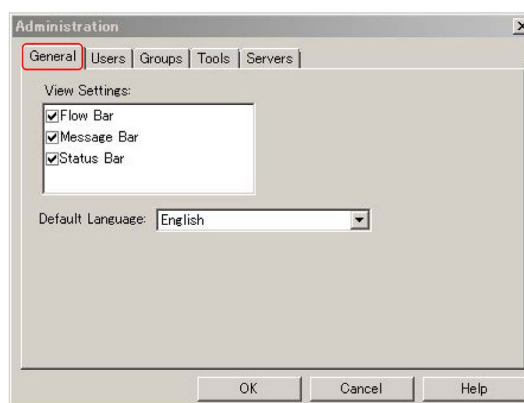


Figure 1.3: AdministrationCGeneral tab.

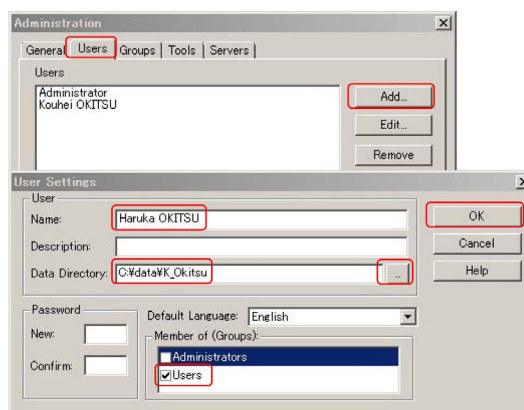


Figure 1.4: Administration, Users tab.

should be clicked after typing the login name 'Administrator' without password. While 'General' tab has been opened as shown in Fig. 1.1, the default settings do not have to be changed. Next, as shown in Fig. 1.2, click 'Administration' in 'Tools' menu, please to display Fig. 1.3. Open 'Users' tab in Fig. 1.4 and click 'Add' button on the upper right corner, please.

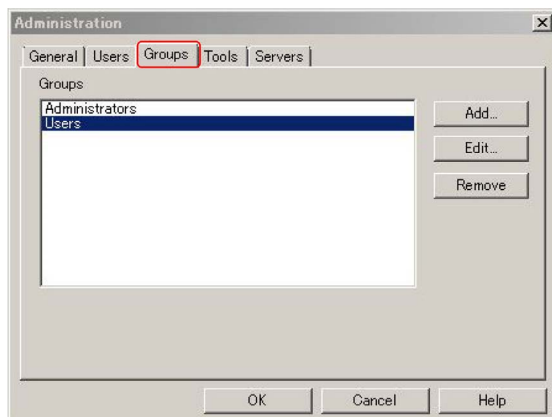


Figure 1.5: AdministrationCGroups tab.

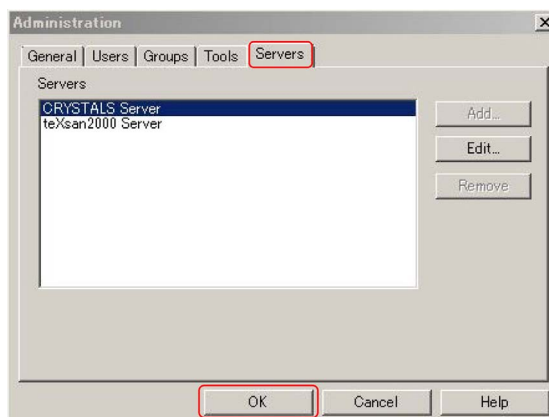


Figure 1.6: AdministrationCServers tab.

Then, 'User Settings' window as shown on the lower part of this figure, opens. 'Name' should be filled with a user name.

The name of laboratory is recommended to be typed only with alphabetical characters. Kanji character cannot be used. Password should not be set. 'Data directory' can be arbitrarily set. However, the name of laboratory is recommended to be set as a new folder in C:\data\.

'...' (browse button) can also be clicked to select or make a folder. Only 'Users' should be checked in 'Member of (Groups)'. In Fig. 1.5 'Group' tab has been opened. 'Add' button can be clicked to make a new group in the same user name. In Fig. 1.6, 'Servers' tab has been opened. After selecting 'CRYSTALS Server', click 'OK' button, please. After that, close the window of 'CrystalStructure', please.

Chapter 2

Determination of molecular structure with ‘CrystalStructure’

Login by double-clicking the icon of ‘CrystalStructure’ on the desktop with the login name, please.

Procedures in ‘[2] Flow chart’ in Fig. 0 on the cover of this manual should be done from up to down.

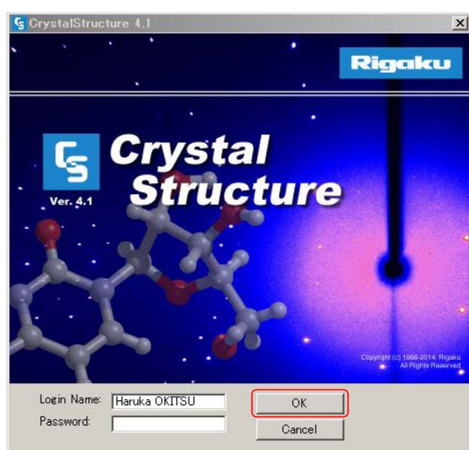


Figure 2.1: Login window.

2.1 Open Project

It is recommended to copy the folder where *.cif_od and other files created by CryAlis^{Pro} exist and to rename it. It should be opened by clicking ‘Open Project’ on the flow chart of CrystalStructure to display a file explorer as shown in Fig. 2.2. Here, ‘Open’ in the lower left corner of Fig. 2.2 should be clicked after selecting ‘*.cif_od’ to display a text window as shown in Fig. 2.3.

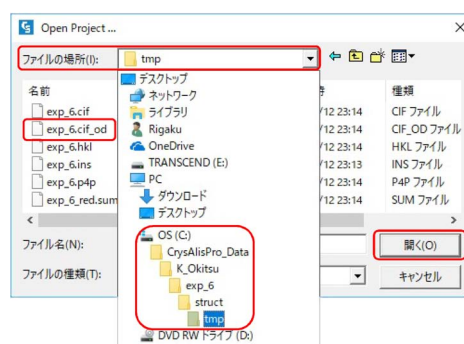


Figure 2.2: Project open

```
Summary for xcalibur
Formula: C12 O11 H22

***** Unit Cell Parameters *****      ***** Model Refinement *****
a: 7.75507(18)                            R1 factor[I>2.0sigma(I)]: 0.0000
b: 8.70250(19)                            R factor[all data]: 0.0000
c: 10.8599(2)                             wR factor[all data]: 0.0000
alpha: 90.000                             goodness of fit: 0.000
beta: 102.940(2)                          # of observations: 0
gamma: 90.000                              # of variables: 0
volume: 714.31(3)                         refl/para ratio: 0.0
                                           maximum shift/error: 0.00
                                           Refinement program: CRYSTALS
                                           Refinement mode: Single
                                           Flack Parameter: 0.000

***** Space Group Information *****    ***** Reflection Corrections *****
symbol: None                              absorption applied: Yes
number: 0                                 abs. type: SYM
centricity: unknown                       abs. range: 0.878-1.000
Z value: 4                                 decay applied: No
Formula weight: 342.30                    decay (%): 0.00
calculated density: 3.183                 redundants averaged: No
mu (cm-1): 2.845
crystal system: monoclinic
laue group: 2/m
lattice type: P

***** Reflection Processing *****      ***** Experimental Information *****
total # processed: 10071                  radiation: Mo
total # unique: 0                        wavelength: 0.71073
R merge (%): 0.00                         max. 2theta: 0.0
Wilson B: 0.00                            sin(theta)/lambda: 0.0000
                                           temperature (C): 23.0
```

Figure 2.3: Text shown after opening the project

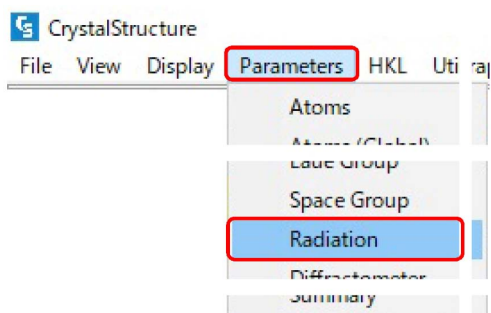


Figure 2.4: X-ray setting menu

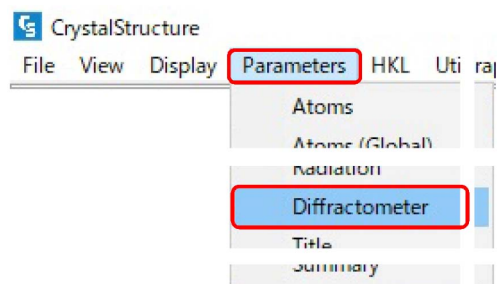


Figure 2.6: Set of the diffractometer

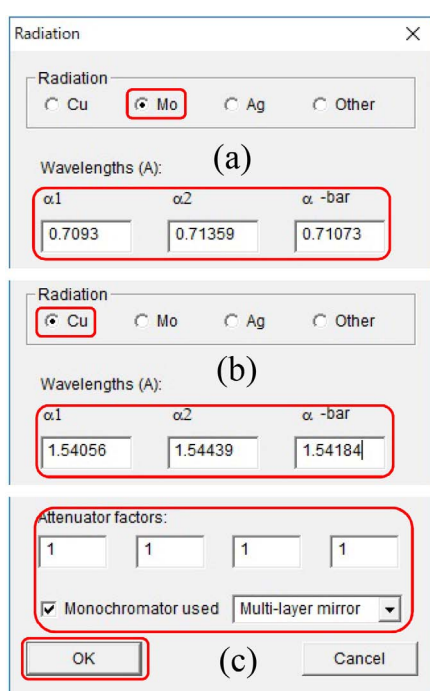


Figure 2.5: X-ray setting should be changed

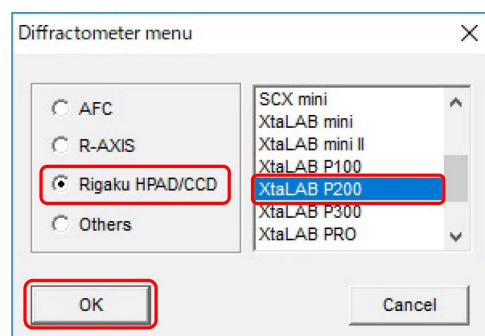


Figure 2.7: Set of the diffractometer and detector

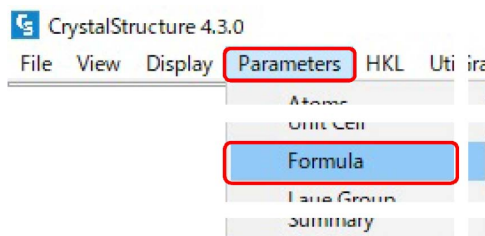


Figure 2.8: Set of the molecular formula

2.2 Change of the parameters

2.2.1 Setting of the X-rays

On the menu bar of CrystalStructure, 'Parameter' can be clicked to display Figs. 2.4, 2.6 and 2.8.

As shown in Fig. 2.5 (a) and (c) for Mo and (b) and (c) for Cu, the wavelength in (a) and (b), the attenuator factors and the used monochromator in (c) should be set.

2.2.2 Setting the diffractometer and the detector

As shown in Fig. 2.6, 'Diffractometer' should be clicked to open a window as shown in Fig. 2.7. 'Rigaku HPAD/CCD' and 'XtaLAB P200' should be selected and then click 'OK'.

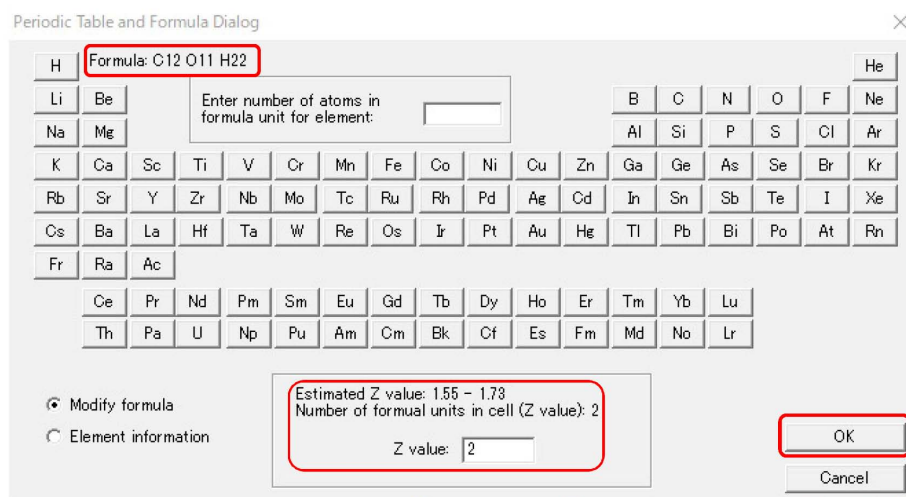


Figure 2.9: Setting the molecular formula and Z value

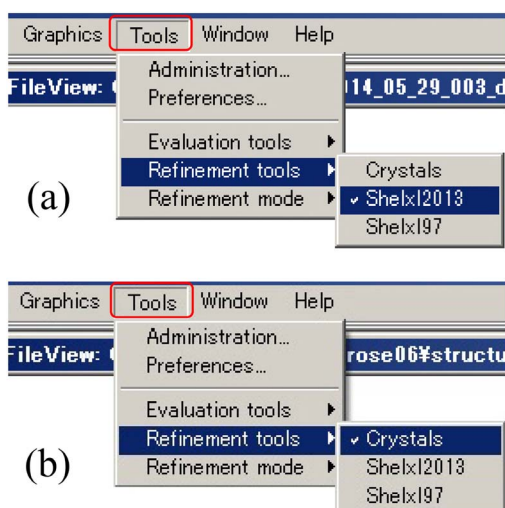


Figure 2.10: Selection of refinement tools.

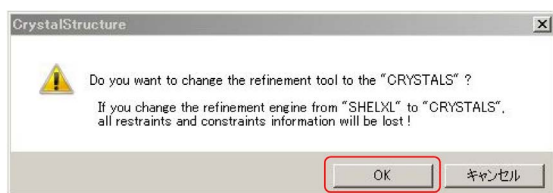


Figure 2.11: Verification message for changing refinement tools.

2.2.3 Change of the value of Z

'Formula' in Fig. 2.8 can be clicked to open the periodic table of the elements in Fig. 2.9. If the molecular formula shown on the upper left corner is wrong, it should be changed by clicking the element and then typing the number of atoms in a molecule to click 'OK' on the lower right corner.

Since 1.55-1.73 is suggested as the estimated Z value on the central lower part of Fig. 2.9, the nearest natural number '2' should be input as the Z number. Z should be corrected because '4' displayed in a red frame in Fig. 2.3 is wrong.

2.3 Selection of the refinement tools

Figure 2.10 shows a window opened by clicking 'Refinement tools' submenu in 'Tools' menu on the menu bar in CrystalStructure 4.1. 'Shelx2013' has been selected as default as shown in Fig. 2.10 (a). However, 'Crystal' can also be selected as shown in Fig. 2.10 (b). If the refinement tool is changed to be 'Crystals', a window as shown in Fig. 2.11 is displayed, in which 'OK' button should be clicked to continue.

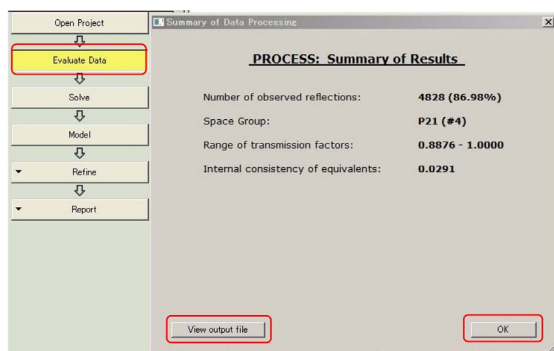


Figure 2.12: Message for average and absorption correction.

After determination of initial phases, the obtained molecular structure should be refined, about which refer to description in §2.6 [p.9], please. ‘Shelx2013’ is a newest tool and then has sophisticated functions such that many procedures can automatically be done. On the other hand, referring to the usage of ‘Crystals’, the sequence of refinement can roughly be grasped. In §2.6 [p.9], the usage of ‘Crystals’ is mainly described. However, referring to this description, ‘Shelx2013’ can also be understood to use.

2.4 Preprocessing measured data

2.4.1 Averaging equivalent diffraction data

‘Evaluate Data’ button in the flow chart (on the upper left corner of Fig. 2.12) can be clicked to open Fig. 2.12.

In an old version ‘CrystalStructure 4.0’, There was ‘Average and absorption correction’ button in the central lower part in Fig. 2.12. This has been abolished in the current version ‘CrystalStructure 4.1’. A message window as shown in Fig. 2.13 has also been abolished such that ‘Weighted average’ and ‘Absorption correction’ are necessarily done.

In an old version ‘CrystalStructure 4.0’, whether averaging ‘Friedel mates’ is done or not, can be selected. However, in the current version ‘CrystalStructure 4.1’, averaging ‘Friedel mates’ is not done. ‘Friedel mate’ is a pair of $h k l$ and $\bar{h} \bar{k} \bar{l}$ reflections. According to Friedel’s law, intensities $h k l$ - and $\bar{h} \bar{k} \bar{l}$ -

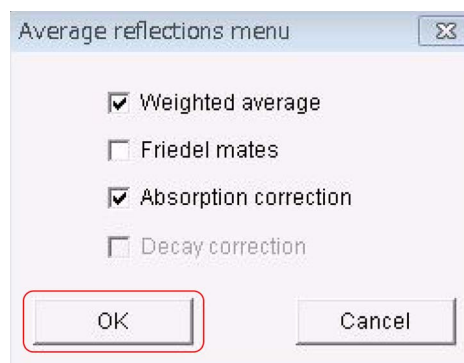


Figure 2.13: Verification message for averaging equivalent diffraction intensities. This message window has been abolished.

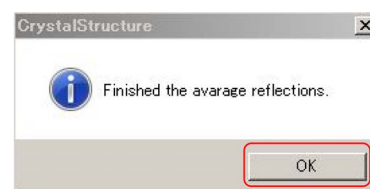


Figure 2.14: Option window for averaging reflections.

reflected X-rays are the same since $|F_{\bar{h} \bar{k} \bar{l}}|^2 = |F_{h k l}^*|^2$. Friedel’s law is satisfied under an assumption that there is no absorption of X-rays in the crystal. However, when the absorption of X-rays is taken into account, it should be assumed that $F_{\bar{h} \bar{k} \bar{l}} \neq F_{h k l}^*$. Then, Friedel’s law is broken. As described later, whether left- or right-handed structure the crystal has (absolute structure), can be estimated from ‘Fleck Parameter’. Since the absorption effect is more significant when using X-rays with long wavelength, Cu $K\alpha$ X-rays are more effective than Mo $K\alpha$ X-rays for determination of the absolute structure. In the old version ‘CrystalStructure 4.0’, in a case of small crystal that includes only light atoms, it was considered that good result can be obtained by averaging Friedel mates, while the information about the absolute structure is lost. However, in the current version, this was abolished such that Fleck parameter is necessarily estimated to determine absolute structure.

By clicking ‘View output file’ button in Fig. 2.12, a text file ‘process.out’ can be displayed of which a part is shown in Figs. B.1 [p.24]

and B.2 [p.24], in which important informations about extinction are described. If space group determined by ‘CrystalStructure’ were wrong, it should be reconsidered referring to Appendix B [p.24].

‘OK’ button in Fig. 2.12 can be clicked to average equivalent reflections to display Fig. 2.14. Here, click ‘OK’ button to continue, please.

2.5 Phase determination and calculation of molecular model

2.5.1 Direct method

In crystal structure analysis, there is a difficulty called ‘phase problem’ that argument (phase) of crystal structure factor cannot be measured while their amplitudes can be directly measured. The direct method is a very strong tool for phase determination developed by Hauptman (Herbert Aaron Hauptman; 1917/2/14-2011/10/23) and Karle (Jerome Karle; 1918/6/18-2013/6/6). It is based on strong restrictions that are given for phases of crystal structure factors by a very evident fact that electron density is positive real function in the crystal. It was rapidly widespread since Karle’s wife (Isabella Karle) coded a computer program for phase determination based on it in 1970’s. Hauptman and Karle was awarded Nobel Prize in Chemistry for this work in 1985.

2.5.2 Phase problem in cases of centrosymmetric crystals

The crystal has symmetric center, the phase problem is very simple, i.e. phases of all structure factors are zero or π (180°). This can easily be understood with the following consideration. The structure factor $F_{\mathbf{h}}$ is defined by

$$F_{\mathbf{h}} = \int_{cell} \rho(\mathbf{r}) \exp[-i2\pi(\mathbf{h} \cdot \mathbf{r})] dv \quad (2.1)$$

$$= \int_{+cell/2} \rho(\mathbf{r}) \exp[-i2\pi(\mathbf{h} \cdot \mathbf{r})] dv + \int_{-cell/2} \rho(-\mathbf{r}) \exp[+i2\pi(\mathbf{h} \cdot \mathbf{r})] dv. \quad (2.2)$$

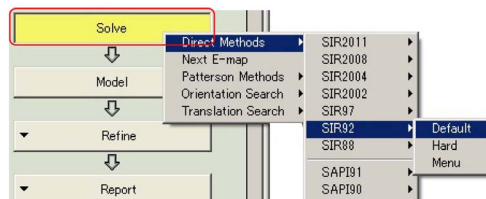


Figure 2.15: Selection of algorithm for phase determination with the direct method.

$\int_{+cell/2} dv$ is a volume integral over half of the unit cell, $\int_{-cell/2} dv$ is a volume integral over the other half of it, $\rho(\mathbf{r})$ is electron density at location \mathbf{r} . $\mathbf{h}(= h\mathbf{a}^* + k\mathbf{b}^* + l\mathbf{c}^*)$ is reciprocal lattice vector giving hkl reflection. With regard to the reciprocal lattice, refer to Appendix A [p.20], please. When the crystal has symmetric center, since $\rho(-\mathbf{r}) = \rho(\mathbf{r})$ when taking it as the origin, contents in integrals of the first and second terms in (2.2) are complex conjugate with each other. Therefore, $F_{\mathbf{h}}$ is necessarily a real value with an argument (phase) of 0 or π (180°).

Symmetric center can frequently be found in cases of racemic crystals that have both right- and left-handed molecules with an identical ratio. In cases of centrosymmetric crystals, the molecular structure can be solved even when the quality of crystal is relatively low. However, effort to obtain a high-quality crystal should be made to decrease the R factor.

When the crystal has only either of left- or right-handed molecules as a protein crystal that consists of only L amino acid, it does not have symmetry center absolutely.

2.5.3 Determination of initial phases with the direct method

As shown in Fig. 0 on the cover of this manual, the molecular structure can sometimes be solved just by clicking ‘[1] Auto’ button automatically to phase crystal structure factors. However, this is a fortunate case. In general, a phase determination algorithm should usually be chosen to obtain initial phases.

The following description is written under an assumption that ‘SIR92’ is selected.

In Fig. 2.15, ‘SIR92’ has been selected as a phase determination algorithm. ‘Default’ can


```

Messages:
CRYSTALS DONE
SolveStructure WorkDir = C:\data\K_Okitsu\
Solve structure successful
    
```

Figure 2.16: Success message of phase determination.

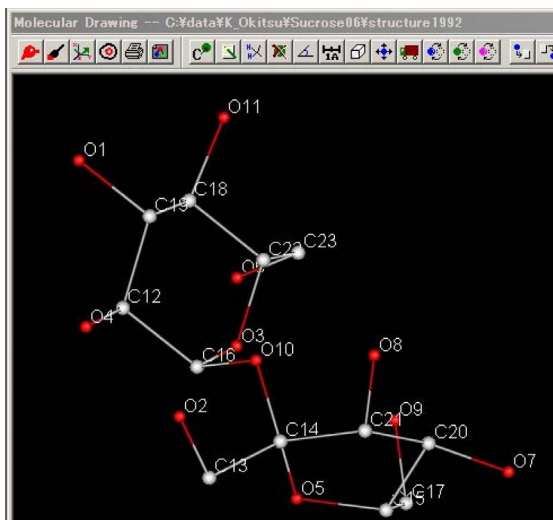


Figure 2.17: Molecular model of solved structure.

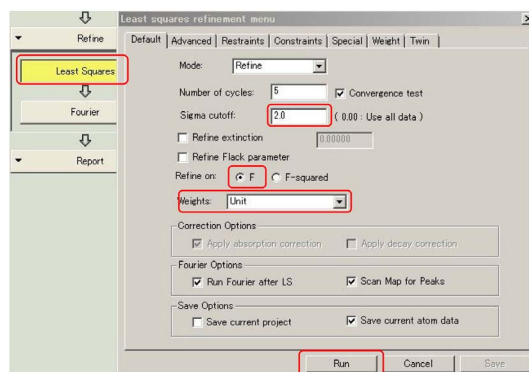


Figure 2.19: Least square fitting window (Crystals).

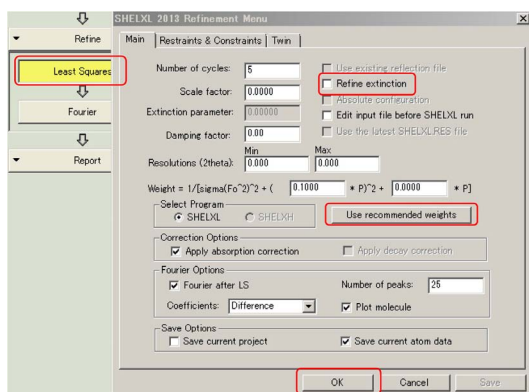


Figure 2.18: Least square fitting window (Shelx).

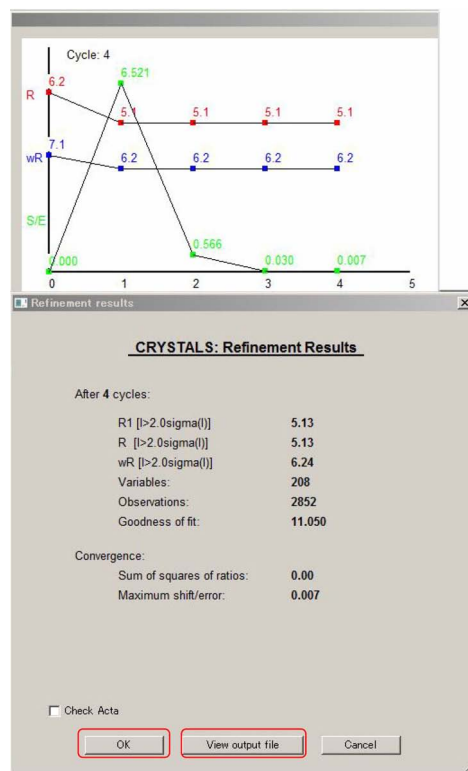


Figure 2.20: Situation of least-square fitting.

```

PRINTER connected to refine.out
Checking SPECIAL positions subject to tolerance of .60000
Refinement directives (LIST 12) processed to activate const
Floating origin in y direction

Refinement of 93 parameters in 1 block(s)
requiring 4573 elements for the least squares matrix - 1

Space required on DISK is 9 records, 36 Blocks,

1 Symmetry restraints written to LIST 17

Sucrose06

Structure factor least squares calculation number 5

Bad agreements

h k l Fo Fc
4. -8. 0. 3.37 2.78
6. -8. 0. 3.19 4.36
6. -6. 0. 3.17 4.07
9. -4. 0. 5.91 7.29
3. -1. 0. 3.04 2.18
3. 0. 0. 37.97 44.59
9. 0. 0. 6.61 7.89
3. 1. 0. 3.23 2.17
7. 2. 0. 14.93 17.50

```

Figure 2.21: Text window showing fitness of the least square fitting.

be clicked to start the process of phase determination. Newer versions of ‘SIR’ have higher functions but is time-consuming.

Figure 2.16 is a message found in bottom part of CrystalStructure window that the crystal structure has been solved successfully by obtaining initial phases. Figure 2.17 in which the obtained molecular structure is shown, can be found by minimizing the white text window. If molecular structure cannot be solved by using ‘SIR92’ with ‘Default’ option, try it again with ‘Hard’ option. When it does not go well, try newer versions of ‘SIR’, please.

If the initial phases were not determined by using ‘SIR’, space group should be reconsider referring to Appendix B [p.24]. In such a case, ‘CrystalStructure’ is recommended to be finished. Retry the procedure described in §2.1 [p.3] after copying five files, ‘CrystalClear.cif’, ‘f2plus.dat’, ‘shelx.hkl’, ‘shelx.p4p’ and ‘texray.inf’ into another new folder.

2.6 Optimization of the molecular structure

2.6.1 Optimization with isotropic temperature factors

‘Refine’ button on the flow chart can be clicked to open ‘Least Squares’ and ‘Fourier’ submenu. ‘Least Squares’ can be clicked to display Fig. 2.18 or 2.19 depending on which ‘Shelx2013’ or ‘Crystals’ is selected as the refinement tool.

In the case of ‘Shelxl2013’, the usage is easier than ‘Crystals’ since the refinement is automatically done only by clicking ‘OK’ button after clicking ‘Use recommended weights’ button. When R factor decreases sufficiently using ‘Shelxl2013’, ‘Refine extinction’ check box in Fig. 2.18 should be checked. However, if R factor increases by checking ‘Refine extinction’, refinement should be done again without checking ‘Refine extinction’.

The following description is mainly given under an assumption that ‘Crystals’ has been chose as the refinement tool as shown in Fig. 2.10 (b) [p.5].

In the case of ‘Crystals’, at first, Click ‘Run’ button after set 2.0 for ‘Sigma cutoff’, F for ‘Refine on’ and Unit for ‘Weights’. Result of least-square fitting is displayed as shown in Fig. 2.20. After repeating this procedure several times, ‘Sigma cutoff’ should be changed to be 0.00.

‘View output file’ button in Fig. 2.20 can be clicked to display refinement results as shown in Fig. 2.21 [p.9] in which reflection indices of which the discrepancy between the absolute value of observed structure factor $|F_o|$ and that calculated based on the structure model $|F_c|$ are summarized. Green spheres found in Fig. 2.22 [p.10] shows positions of peaks that are not assigned for atoms. These can be hidden by clicking ‘[1] Peak ON/OFF’ button.

2.6.2 Optimization with anisotropic temperature factors

‘Refinement Attributes’ appearing clicked by ‘Model’ button in the flow chart as shown in Fig. 2.23, can be clicked to display Fig. 2.24. Here, ‘xyz’ and ‘aniso’ should be checked such that optimization of xyz coordinates and

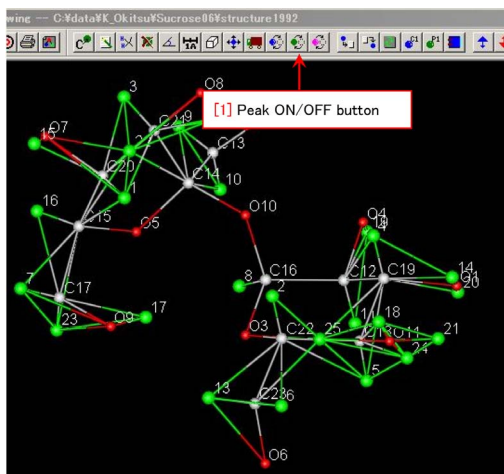


Figure 2.22: Green spheres can be hidden by clicking '[1] Peak ON/OFF' button.

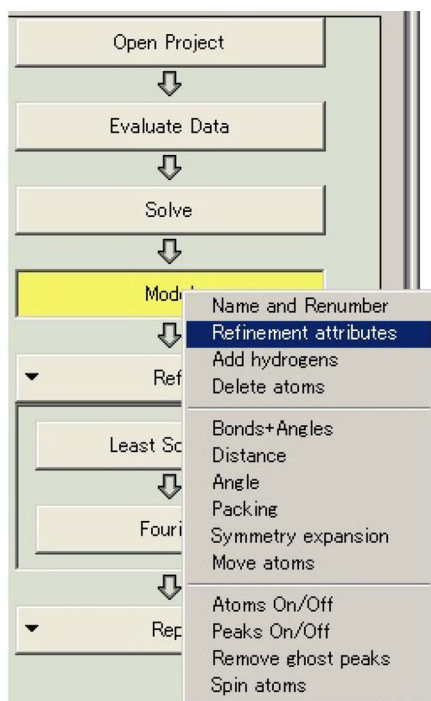


Figure 2.23: 'Refinement attributes' should be clicked.

anisotropic temperature factor are applied. After clicking 'All non-hydrogen' button, 'Apply' button can be checked to apply the checked conditions to all no-hydrogen atoms as shown in Fig. 2.25

'OK' button can be clicked such that atoms in the molecular model are displayed as cubes as shown in Fig. 2.26. The same procedure as for isotropic temperature factors can be done to display Fig. 2.27. Here, 'OK' button can be clicked to continue.

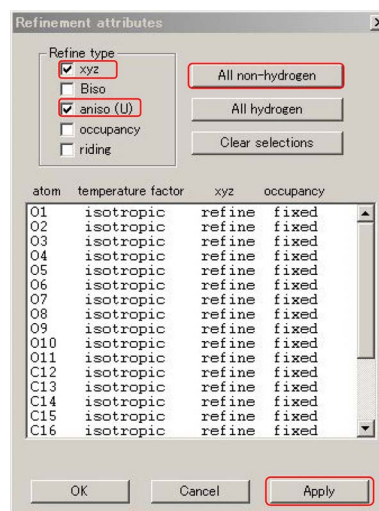


Figure 2.24: Position refinement and anisotropic temperature factor are applied for non-hydrogen atoms.

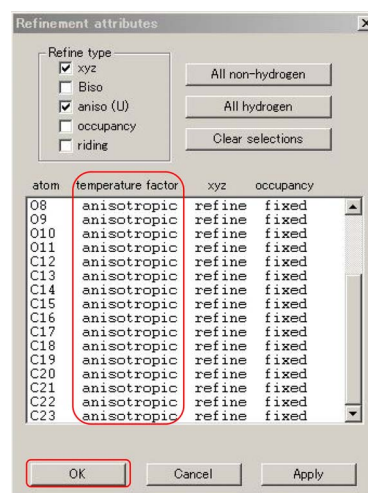


Figure 2.25: Anisotropic temperature factors have been applied for non-hydrogen atoms.

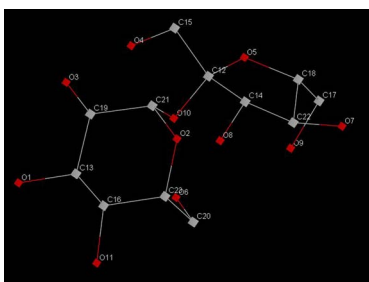


Figure 2.26: Shapes of non-hydrogen atoms changed to be cubes.

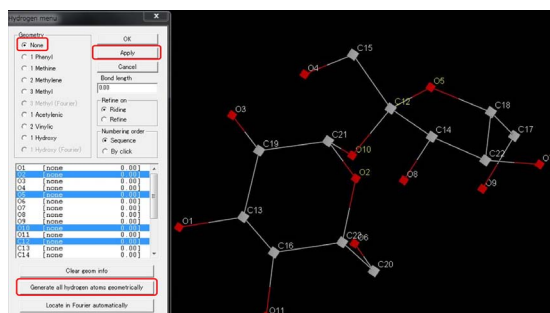


Figure 2.29: Selection of atoms with no hydrogen.

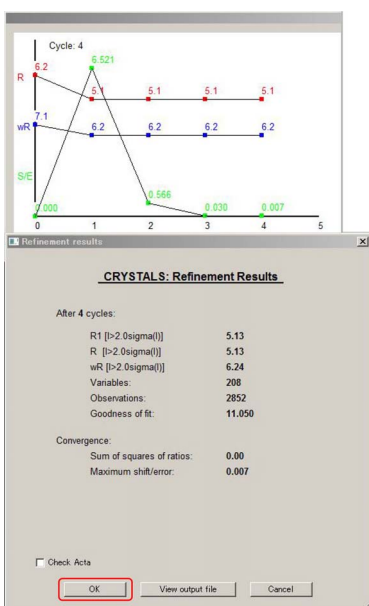


Figure 2.27: Window showing the fitting situation.

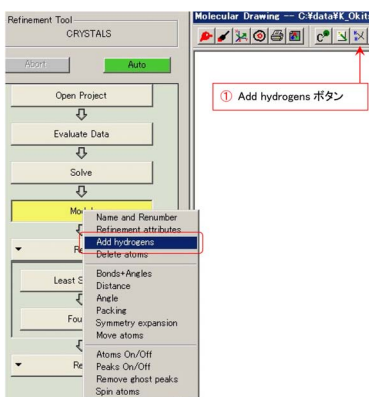


Figure 2.28: Process of fitting with hydrogen atoms.

2.7 Optimization taking into account hydrogen atoms

2.7.1 Automatic assignment of hydrogen atoms

Figure 2.28 can be displayed by clicking 'Model' button in the flow chart. '[1] Add hydrogens' button in Fig. 2.28 can be clicked to display Fig. 2.29. The same result is given by clicking 'Add hydrogens' in the menu appearing with 'Model' button in the flow chart clicked in Fig. 2.28. In fortunate cases, All hydrogen atoms can be automatically assigned just by clicking 'Generate all hydrogen atoms geometrically' button in Fig. 2.29. In general, hydrogen atoms should be assigned by considering solid geometrical configuration of the molecular model.

2.7.2 Manual assignment of hydrogen atoms

After checking 'None' radio button as shown in Fig. 2.29 [p.11], atoms considered to be bonded with no hydrogen should be clicked. Then, click 'Apply' button, please. Next, after clicking 'Hydroxy' radio button in Fig. 2.30, atoms that are considered to be hydroxyl oxygen should be clicked and then click 'Apply' button, please.

Similarly, atoms of methine carbon and methylene carbon should be selected by clicking as shown in Figs. 2.31 and 2.32. After all non-hydrogen atoms are assigned, 'OK' button should be clicked to display Fig. 2.33.

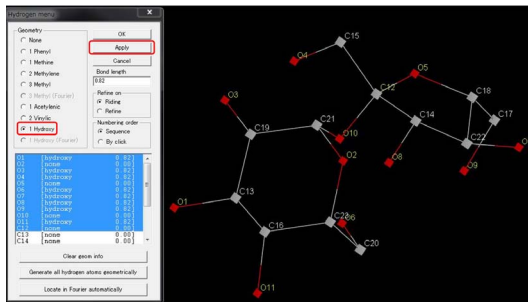


Figure 2.30: Selection of hydroxyl oxygens.

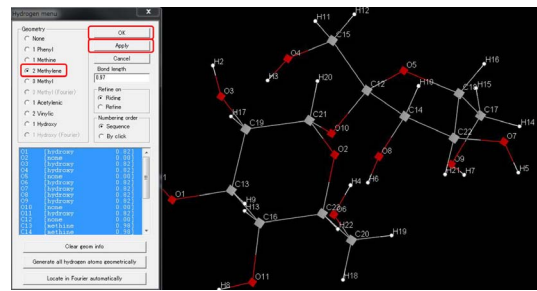


Figure 2.33: All hydrogen atoms have been assigned.

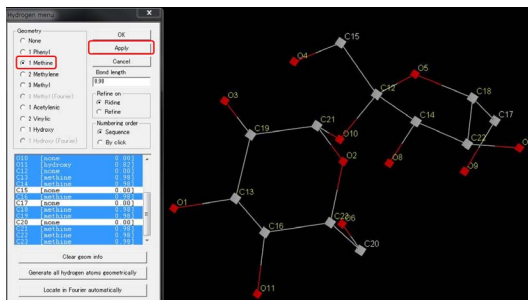


Figure 2.31: Selection of methine carbon.

2.7.3 Execution of least square fitting

'Model' button in the flow chart should be clicked to display Fig. 2.34. Here, 'Refinement attributes' should be clicked to display Fig. 2.35.

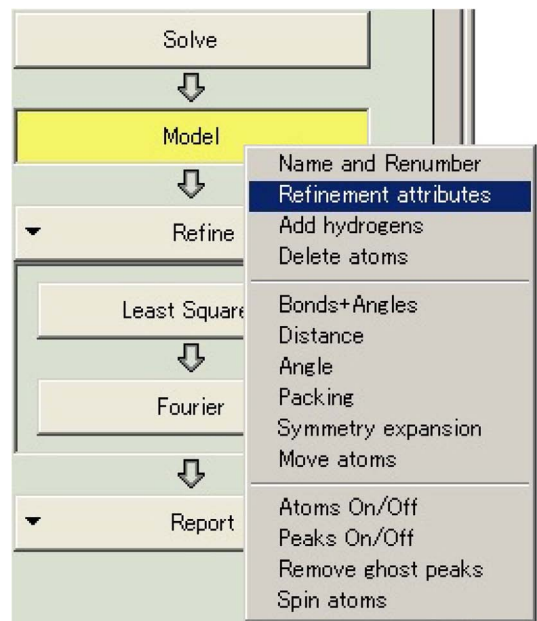


Figure 2.34: Refinement settings.

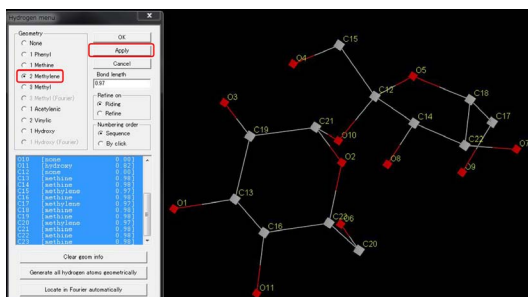


Figure 2.32: Selection of methylene carbon.

Here, after checking only 'xyz' check box, 'All hydrogens' buttons and then 'Apply' button can be clicked such that positions of all hydrogen atoms are optimized. Then, click 'OK' button, please.

After clicking 'Refine' button in the flow chart, 'Least squares' button can be clicked to display Fig. 2.36. After setting 0.00 for

atom	temperature factor	xyz	occupancy
H7	fixed	refine	fixed
H8	fixed	refine	fixed
H9	fixed	refine	fixed
H10	fixed	refine	fixed
H11	fixed	refine	fixed
H12	fixed	refine	fixed
H13	fixed	refine	fixed
H14	fixed	refine	fixed
H15	fixed	refine	fixed
H16	fixed	refine	fixed
H17	fixed	refine	fixed
H18	fixed	refine	fixed
H19	fixed	refine	fixed
H20	fixed	refine	fixed
H21	fixed	refine	fixed
H22	fixed	refine	fixed

Figure 2.35: Refinement settings for hydrogen positions.

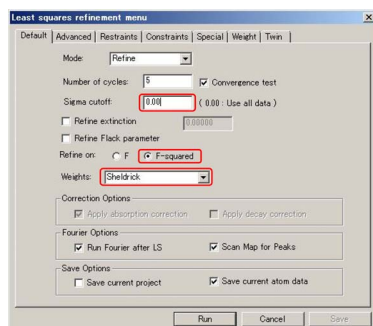


Figure 2.36: Refinement settings with ‘Sheldrick’ weights.

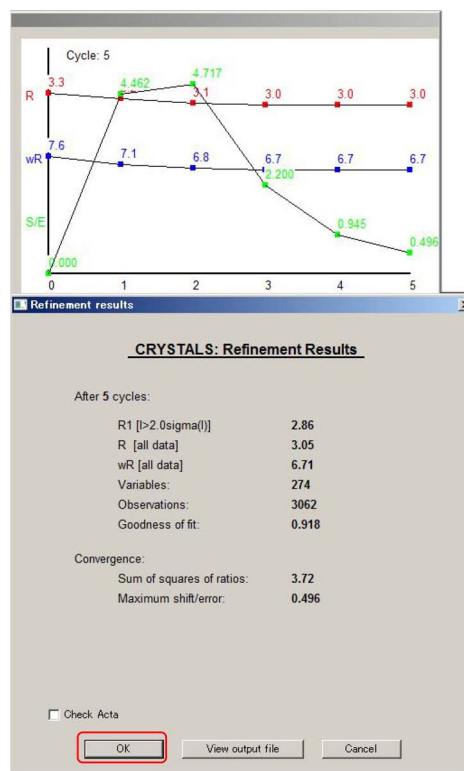


Figure 2.38: Refinement results.

‘Sigma cutoff:’, ‘F-squared’ for ‘Refine on:’ and ‘Sheldrick’ for ‘Weights:’, ‘Weights’ tab should be opened as shown in Fig. 2.37. ‘Calculate values’ button can be clicked such that ‘Weights:’ used when doing least square fitting is calculated and displayed. Here, ‘OK’ button and then ‘Run’ button can be clicked to display the result of least square fitting as shown in Fig. 2.38.

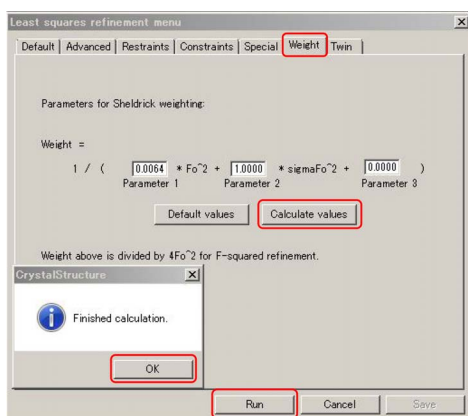


Figure 2.37: Calculation of weights.

Open ‘Weight’ tab again as shown in Fig. 2.37 in the refinement setting window and then click ‘Calculate values’ button to display Fig. 2.39 [p.14], please. By clicking ‘OK’ button, ‘Default’ tab is found to be opened as shown in Fig. 2.40 [p.14]. Here, parameters should be set as in this figure.

Note that ‘Refine extinction’ and ‘Flack

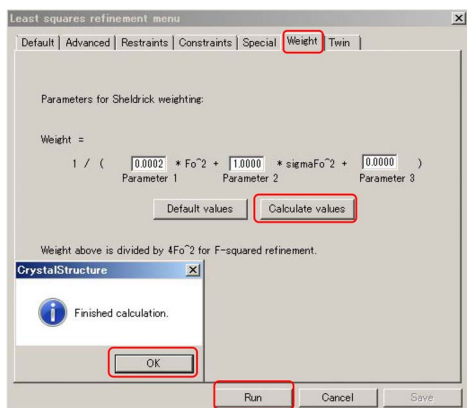


Figure 2.39: Calculation of weights (again).

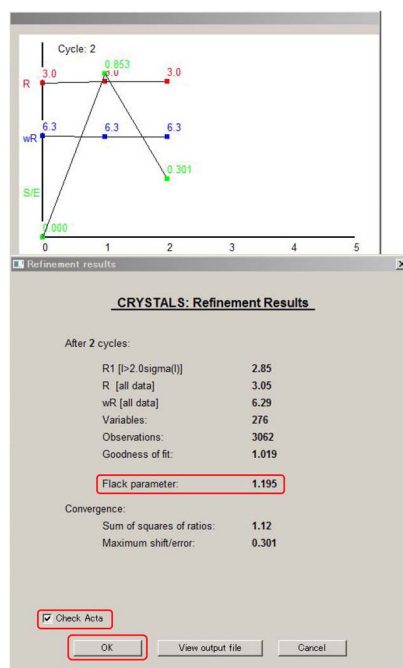


Figure 2.41: Refinement results (again).

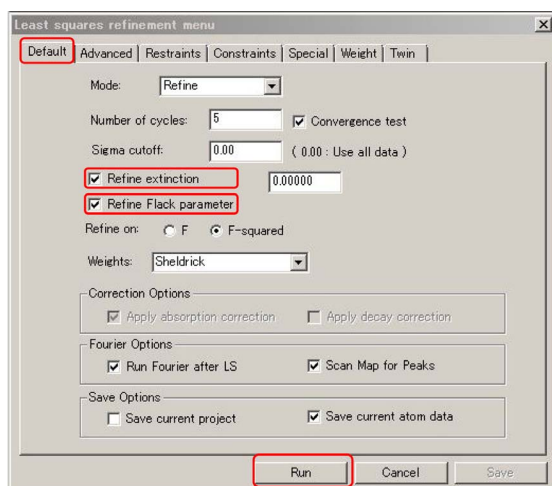


Figure 2.40: Refinement settings (again).



Figure 2.42: Checking window for publication in Acta Cryst. C (#1).

Parameter' have been checked. 'Extinction effect' is a phenomenon that reflected X-ray intensity decreases due to dynamical diffraction effect. 'Flack parameter' is a parameter in a range of $0 \sim 1$ that indicates whether correct or not the obtained absolute structure is. Least square fitting can be started by clicking 'Run' button to display Fig. 2.41. Smaller deviation of 'Flack parameter' from 0 than from 1 means that the obtained absolute structure is right with a high possibility. The value 0.833 as 'Flack parameter' shown here means that the absolute structure is not right. Here, check 'Check Acta' for estimating the validity for publication in Acta Cryst. C to click 'OK' button, please.

In Fig. 2.42, the value of 'Max. Shift /



Figure 2.43: Checking window for publication in Acta Cryst. C (#2).

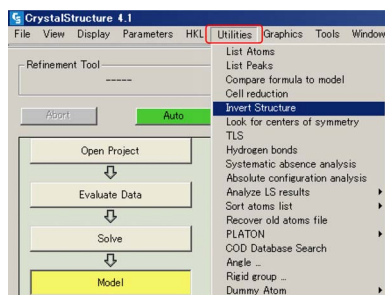


Figure 2.44: Inversion of absolute structure.



Figure 2.46: Checking window for publication in Acta Cryst. C (#4; final).

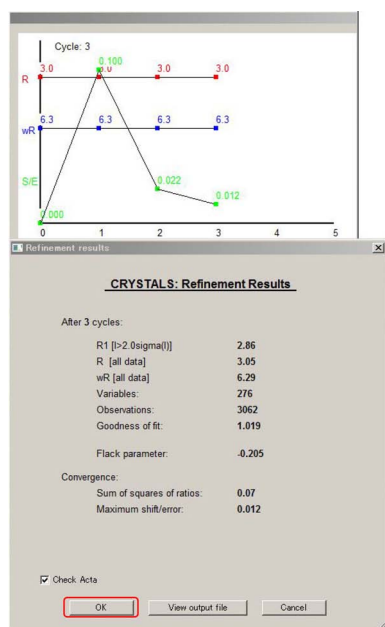


Figure 2.45: Checking window for publication in Acta Cryst. C (#3).

Error' has been displayed with red characters, which means it does not satisfy the validity for publication in Acta Cryst. C. There are three levels of ALART, A, B and C. ALART A means the most severe problem. After repeating the procedures of Figs. 2.39, 2.40 and 2.41 by several times, as shown in Fig. 2.43, the ALART level has come to be B. Here, 'Invert structure' should be clicked in 'Utility' menu in Fig. 2.44 for inverting the molecular structure.

The procedures of Figs. 2.39, 2.40 and 2.41 should be repeated such that 'Max. Shift / Error' is converged to be zero and 'Goodness of fit' approaches to unity until improvement in values of R1 and wR cannot be found. Figure 2.46 is

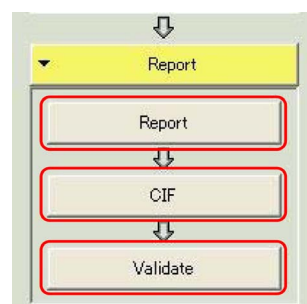


Figure 2.47: 'Report' button has been clicked.

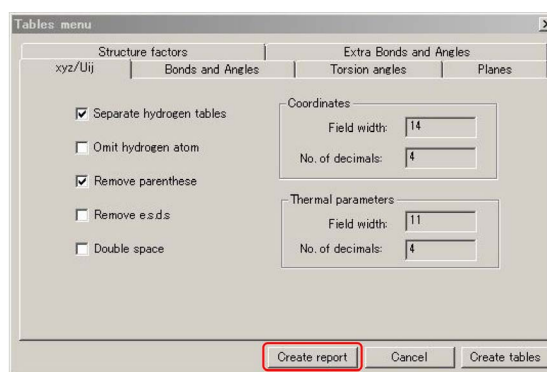


Figure 2.48: Making crystal information file.

displayed when the optimization is completed.

2.8 Making a report

2.8.1 Making an rtf file

'Report' button in the flow chart can be clicked to display 'Report', 'CIF' and 'Validate' as shown in Fig. 2.47. Here, 'Report' can be clicked to display Fig. 2.48.

$a = 7.713(2) \text{ \AA}$
 $b = 8.664(2) \text{ \AA}$
 $c = 10.812(3) \text{ \AA}$
 $V = 704.0(4) \text{ \AA}^3$

$\beta = 103.014(5)^\circ$

For $Z = 2$ and $F.W. = 342.30$, the calculated density is 1.615 g/cm^3 . Based on the reflection conditions of:

Ok0: $k = 2n$

packing considerations, a statistical analysis of intensity distribution, and the successful solution and refinement of the structure, the space group was determined to be:

P2₁ (#4)

Figure 2.49: Crystal information ('*.rtf' file).



Figure 2.50: Making 'Cif.Cif'.

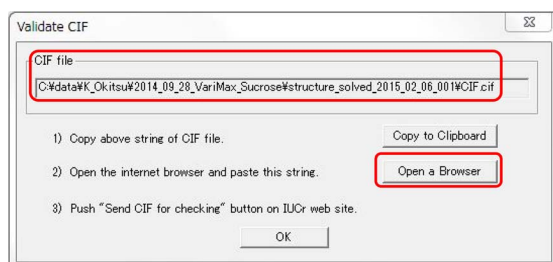


Figure 2.51: 'Open a Browser' button should be clicked.

Then, 'Create report' button can be clicked to make an rtf file in which crystal informations are written partially as shown in 2.49.

2.8.2 Making CIF files

'CIF' button can be clicked to display Fig. 2.50. Here, 'OK' button can be clicked to make 'Cif.Cif' and finish the crystal structure analysis. Then, close the window of 'CrystalStructure', please.

2.9 Loading a CIF file and drawing a molecular model

After starting 'CrystalStructure' again,



Figure 2.52: Start window of 'PLATON'.

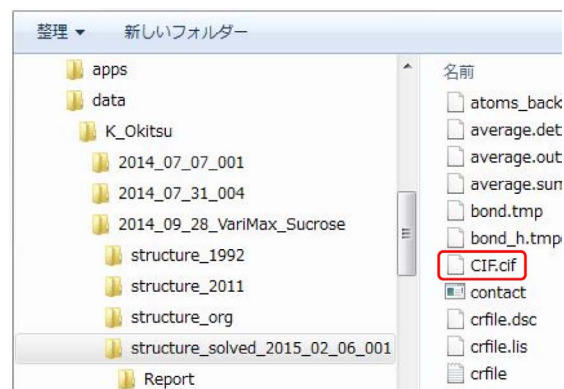


Figure 2.53: 'Cif.cif' should be selected.

'Open Project' button in the flow chart can be clicked to open the folder in which 'Crystal-Clear.Cif' has been placed as shown in Fig. 2.58. Here, 'Cif.Cif' should be selected for loading.

Figure 2.59 [p.18] has been displayed by selecting 'Ball and Stick' from 'Style' submenu in 'Display' menu. The molecular structure is displayed with red (for O), white large (for C) and white small (for H) balls and sticks.

Figure 2.60 [p.18] has been displayed by selecting 'Thermal Ellipsoid' from 'Style' submenu in 'Display' menu. Thermal oscillation of O11 atom is found to be anisotropic.

2.9.1 Check of CIF file

By clicking 'Validate' button in Fig.2.46 [p.15], the analysis result can be checked with a software called 'PLATON' placed on the web site of IUCr. Figure 2.51 is a window displayed by clicking the 'Validate' button in Fig. 2.47 [p.15]. After checking the full path of 'Cif.Cif' in a red flame, 'Open a Browser' button can be



Figure 2.54: ‘Cif.cif’ is sent to IUCr web site by clicking ‘Send CIF for checking’ button.

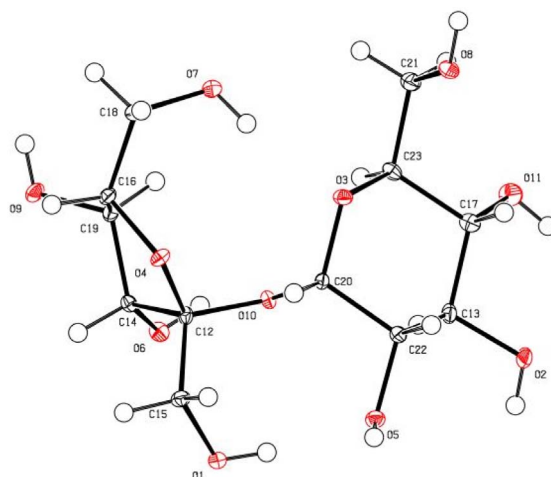


Figure 2.57: Thermal ellipsoid model of molecular structure.

Datablock: Sucrose_2014_09_28_001			
Bond precision:	C-C = 0.0033 Å	Wavelength=0.7107	
Cell:	a=7.712(3)	b=8.662(3)	c=10.812(4)
	alpha=90	beta=102.983(5)	gamma=90
Temperature:	273 K		
Volume	703.8(4)	Calculated	Reported
Space group	F 21		F 1 21 1
Hall group	F 2yb		F 2yb
Moiety formula	C12 H22 O11		C12 H22 O11
Sum formula	C12 H22 O11		C12 H22 O11

Figure 2.55: ‘PLATON’ for checking the molecular structure has been opened.

Alert level A			
PLAT415_ALERT_2_A	Short Inter D-H...H-X	H8 .. H18A ..	1.73 Ang.
PLAT417_ALERT_2_A	Short Inter D-H...H-D	H6 .. H9 ..	1.58 Ang.
Alert level B			
PLAT420_ALERT_2_B	D-H Without Acceptor	O8 - H8 ..	Please Check
Alert level C			
STRVA01_ALERT_2_C	Chirality of atom sites is inverted?		
	From the CIF: _refine_ls_abs_structure_Flack		0.800
	From the CIF: _refine_ls_abs_structure_Flack_su		0.500
PLAT415_ALERT_2_C	Short Inter D-H...H-X	H8 .. H15A ..	2.10 Ang.
PLAT482_ALERT_4_C	Small D-H...A Angle Rep for O6	.. O10 ..	99.50 Degree
Alert level G			
CHEMS02_ALERT_1_G	Please check that you have entered the correct _publ_requested_category classification of your compound;		

Figure 2.56: Alerts on solved molecular structure.

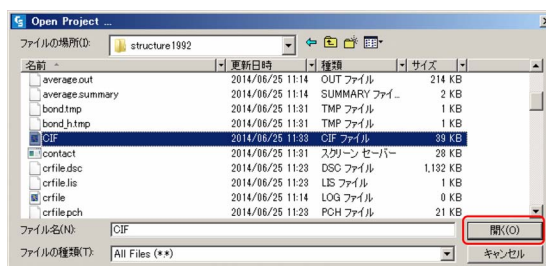


Figure 2.58: Loading ‘Cif.Cif’.

clicked to open a window as shown in Fig. 2.52. By clicking a button in a red flame in Fig. 2.52, an explore window can be opened as shown in Fig. 2.53. In this figure, ‘Cif.cif’ should be double-clicked to select. About 20 seconds after that, a windows as shown in Fig 2.55 is displayed. In a red flame of this figure, lattice parameters, volume of unit cell and space group are described. By slightly scrolling down, items on which reconsideration is recommended are shown as alerts level A, B, C and G as shown in Fig. 2.56. By further scrolling down, as shown in Fig. 2.57, a molecular model can be seen with thermal ellipsoids.

2.9.2 Drawing the molecular model

After restarting ‘CrystalStructure’, click

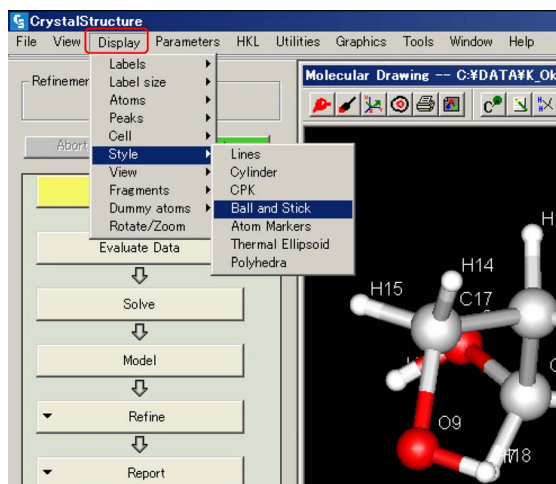


Figure 2.59: Thermal ellipsoid model of molecular structure.

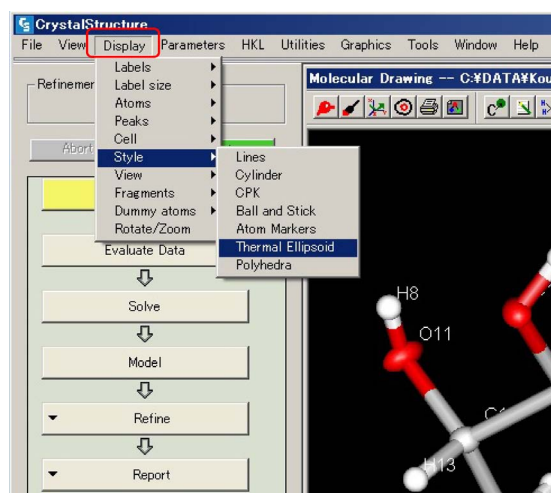


Figure 2.60: Thermal ellipsoid model of molecular structure.

'Open Project' button in the flow chart and then open a folder in which 'Cif.cif' is placed, please to display a window as shown in Fig. 2.58 [p.17]. Here, load 'Cif.cif', please. By clicking 'Ball and stick' in 'Style' submenu in 'Display' menu on the menu bar, the molecular structure

is displayed with balls (O:red, C:gray, H:white) and sticks.

By clicking 'Thermal ellipsoid' in 'Style' submenu in 'Display' menu on the menu bar, Fig. 2.60 can be displayed. An anisotropy of thermal vibration of O11 atom can be observed.

To be continued.

Appendix A

Why should we define ‘Reciprocal Lattice’ ?

For many students working on crystallography, the first difficulty is understanding of reciprocal lattice. In spite that the Bragg condition written by (A.1) or (A.2) can easily be understood, why such strange ideas as reciprocal lattice and reciprocal space should we use ? This chapter describes the equivalence of Bragg’s reflection condition, Laue’s reflection condition and Ewald construction (Reciprocal lattice node exists on the Ewald sphere), from which how reasonably the reciprocal lattice is defined can be understood.

Every space group of crystal has an extinction rule owing to its symmetry with which the crystal structure factor comes to be zero. However, it is neglected in the following description for simplicity.

A.1 Bragg’s reflection condition

Figure A.1 shows Bragg’s reflection condition. This figure is also found in high school text book. Bragg’s reflection condition can relatively easily and intuitively referring to this figure. When atoms (or molecules) are arranged on a set of planes as shown in Fig. A.1. Optical path length of X-rays drawn as a gray line are longer than that drawn as a black line by $|\vec{ab}| + |\vec{bc}| (= 2d \sin \theta_B)$. When this length is an integral multiplication of the wavelength, these rays interfere constructively with each other. Therefore, reflection condition can be described as follows,

$$2d \sin \theta_B = n\lambda. \quad (\text{A.1})$$

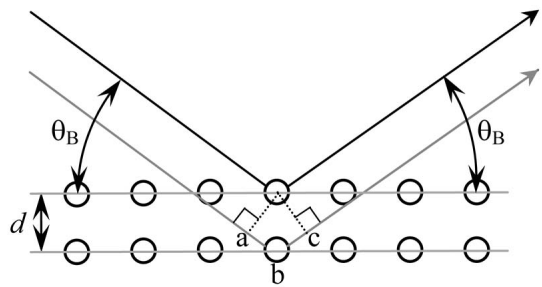


Figure A.1: Bragg’s reflection condition.

By redefining lattice spacing d' to be $d' = d/n$, the following equation is also frequently used,

$$2d' \sin \theta_B = \lambda. \quad (\text{A.2})$$

Now, let us consider why the angle of incidence and emergence is identical. Is it evident since the Bragg plane works as a mirror plane ? Then, why are the angles of incidence and emergence of a mirror identical ? Sometimes, even a veteran of crystallography cannot answer to this question.

A.2 Laue’s reflection condition

Laue’s reflection condition was used to explain the phenomenon of X-ray diffraction when it was invented by Laue (Max Theodor Felix von Laue; 1879/10/9-1960/4/24) in 1912, which is described referring to Fig. A.2 as follows,

$$\begin{aligned} R_0B - AR_1 \\ = \overrightarrow{R_0R_1} \cdot \mathbf{s}_1 - \overrightarrow{R_0R_1} \cdot \mathbf{s}_0 = n_0\lambda. \end{aligned} \quad (\text{A.3})$$

Here, \mathbf{s}_0 and \mathbf{s}_1 are unit vectors in the direction of propagation of incident and reflected X-rays.

When R_0 and R_1 are equivalent lattice points, difference in optical path length between black and gray paths drawn in Fig. A.2 is given by (A.3). When this difference in path length is an integral multiplication of wavelength, X-rays scattered by lattice points R_0 and R_1 interfere constructively with each other.

Incidentally, since R_0 and R_1 are equivalent lattice point, there is a restriction as follows,

$$\overrightarrow{R_0R_1} = n_1\mathbf{a} + n_2\mathbf{b} + n_3\mathbf{c}, \quad (\text{A.4})$$

where, n_1 , n_2 and n_3 are arbitrary integers. \mathbf{a} , \mathbf{b} and \mathbf{c} are primitive translation vectors. That is to say the left hand side of (A.3) should be integral multiplication of wavelength for arbitrary integers n_1 , n_2 and n_3 . Lattice points R_0 and R_1 can move freely with a restriction that these are equivalent points. The value of left hand side of (A.3) is evidently positive when $\overrightarrow{R_0R_1} \cdot \mathbf{s}_1 > \overrightarrow{R_0R_1} \cdot \mathbf{s}_0$ and is negative when $\overrightarrow{R_0R_1} \cdot \mathbf{s}_1 < \overrightarrow{R_0R_1} \cdot \mathbf{s}_0$. Figure A.2 is drawn under an assumption of the latter case.

However, R_0 and R_1 can also be taken such that $\overrightarrow{R_0R_1} \cdot \mathbf{s}_1 = \overrightarrow{R_0R_1} \cdot \mathbf{s}_0$. In the following discussion in this paragraph, R_0 and R_1 are fixed such that $\overrightarrow{R_0R_1} \cdot \mathbf{s}_1 = \overrightarrow{R_0R_1} \cdot \mathbf{s}_0$. When R_0 , R_1 and optical paths drawn as black and gray lines are all on the drawing, there should be a plane perpendicular to the drawing that include those points and optical paths. When X-rays are scattered at any point on this plane under a condition that the angles of incidence and emergence are the same, the optical path length is always the same. This is also the reason for that the angle of incidence and emergence for a mirror is always identical.

In Bragg's reflection condition, under an implicit (the first and second dimensional) restriction that optical path length are always the same for a defined Bragg plane when the angle of incidence and emergence is identical, the third dimensional condition is given by (A.1) or (A.2). Behind the simple condition given by those equations, the above mentioned first and second dimensional restrictions are hidden.

Now, for description in the next section, the following equation is prepared by dividing the both sides of eq. (A.3) by the wavelength λ ,

$$\overrightarrow{R_0R_1} \cdot \left(\frac{\mathbf{s}_1}{\lambda} - \frac{\mathbf{s}_0}{\lambda} \right) = n_0. \quad (\text{A.5})$$

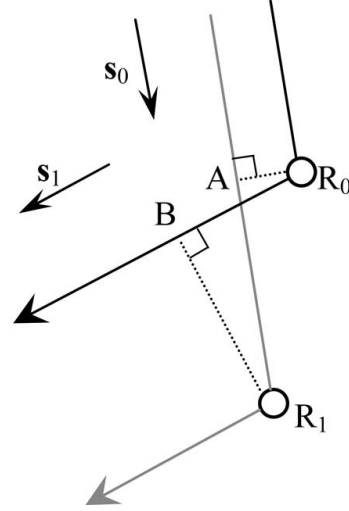


Figure A.2: Laue's reflection condition.

By substituting (A.4) into the above equation and considering that the wave vectors of incident and reflected X-rays are given by $\mathbf{K}_0 = \mathbf{s}_0/\lambda$ and $\mathbf{K}_1 = \mathbf{s}_1/\lambda$, the following equation can be obtained,

$$(n_1\mathbf{a} + n_2\mathbf{b} + n_3\mathbf{c}) \cdot (\mathbf{K}_1 - \mathbf{K}_0) = n_0. \quad (\text{A.6})$$

A.3 Ewald's reflection condition (Ewald construction)

A.3.1 Foundation of Ewald construction

Fig. A.3 [p.22] shows the situation that the origin O of reciprocal space and a reciprocal lattice node H_{hkl} simultaneously exist on the surface of Ewald sphere. Its center is the common initial point of wave vectors \mathbf{K}_0 and \mathbf{K}_1 .

In the description of Ewald construction, at first, reciprocal fundamental vectors \mathbf{a}^* , \mathbf{b}^* and \mathbf{c}^* are defined as follows:

$$\mathbf{a}^* = \frac{\mathbf{b} \times \mathbf{c}}{\mathbf{a} \cdot (\mathbf{b} \times \mathbf{c})}, \quad (\text{A.7a})$$

$$\mathbf{b}^* = \frac{\mathbf{c} \times \mathbf{a}}{\mathbf{a} \cdot (\mathbf{b} \times \mathbf{c})}, \quad (\text{A.7b})$$

$$\mathbf{c}^* = \frac{\mathbf{a} \times \mathbf{b}}{\mathbf{a} \cdot (\mathbf{b} \times \mathbf{c})}. \quad (\text{A.7c})$$

The denominator of (A.7), $\mathbf{a} \cdot (\mathbf{b} \times \mathbf{c})$ [= $\mathbf{b} \cdot (\mathbf{c} \times \mathbf{a}) = \mathbf{c} \cdot (\mathbf{a} \times \mathbf{b})$] is the volume of parallelepiped whose edges are \mathbf{a} , \mathbf{b} and \mathbf{c} . From

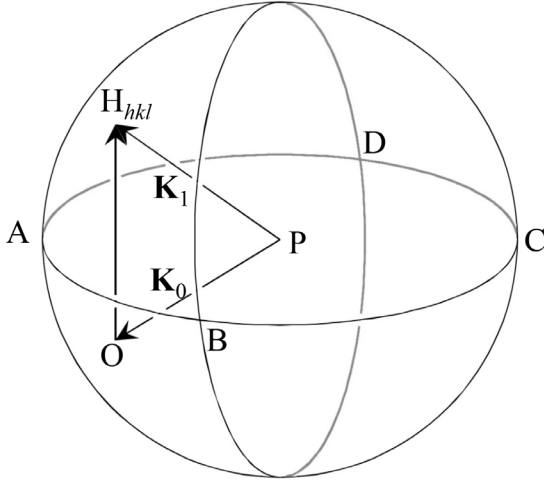


Figure A.3: Ewald sphere

the above definitions, the following equations are evident,

$$\mathbf{a} \cdot \mathbf{a}^* = 1, \quad (\text{A.8a})$$

$$\mathbf{b} \cdot \mathbf{b}^* = 1, \quad (\text{A.8b})$$

$$\mathbf{c} \cdot \mathbf{c}^* = 1. \quad (\text{A.8c})$$

Further, $\mathbf{b} \times \mathbf{c}$ is a vector that is perpendicular to both \mathbf{b} and \mathbf{c} and has a length of the area of parallelogram whose sides are \mathbf{b} and \mathbf{c} . Here, vectors \mathbf{b} , \mathbf{c} and $\mathbf{b} \times \mathbf{c}$ construct a right-handed system. Since the above is the same for $\mathbf{c} \times \mathbf{a}$ and $\mathbf{a} \times \mathbf{b}$, the following relations are also evident,

$$\mathbf{a} \cdot \mathbf{b}^* = \mathbf{a} \cdot \mathbf{c}^* = 0, \quad (\text{A.9a})$$

$$\mathbf{b} \cdot \mathbf{c}^* = \mathbf{b} \cdot \mathbf{a}^* = 0, \quad (\text{A.9b})$$

$$\mathbf{c} \cdot \mathbf{a}^* = \mathbf{c} \cdot \mathbf{b}^* = 0. \quad (\text{A.9c})$$

That is to say, \mathbf{a}^* , \mathbf{b}^* and \mathbf{c}^* have been defined such that (A.8) and (A.9) are satisfied.

A reflection vector giving $h k l$ reflection is defined in general as follows:

$$\overrightarrow{\text{OH}}_{hkl} = h\mathbf{a}^* + k\mathbf{b}^* + l\mathbf{c}^*. \quad (\text{A.10})$$

Here, O is the origin of reciprocal space. The Ewald sphere is a sphere whose center is P. The wave vector of the incident X-rays \mathbf{K}_0 is $\overrightarrow{\text{PO}}$. When a reciprocal lattice node H_{hkl} exists on the surface of the Ewald sphere, reflected X-rays whose wave vector \mathbf{K}_1 is $\overrightarrow{\text{OH}}_{hkl}$ are excited. Then, the following equation is satisfied,

$$\begin{aligned} \mathbf{K}_1 - \mathbf{K}_0 &= \overrightarrow{\text{OH}}_{hkl} \\ &= h\mathbf{a}^* + k\mathbf{b}^* + l\mathbf{c}^*. \end{aligned} \quad (\text{A.11})$$

Let us calculate the left-hand side of (A.6) [p.21] by substituting (A.11) into the second term of the left-hand side of (A.6) [p.21] and considering (A.8) and (A.9) as follows:

$$\begin{aligned} (n_x\mathbf{a} + n_y\mathbf{b} + n_z\mathbf{c}) \cdot (\mathbf{K}_1 - \mathbf{K}_0) \\ = (n_x\mathbf{a} + n_y\mathbf{b} + n_z\mathbf{c}) \cdot (h\mathbf{a}^* + k\mathbf{b}^* + l\mathbf{c}^*) \end{aligned} \quad (\text{A.12})$$

$$= n_x h + n_y k + n_z l. \quad (\text{A.13})$$

Since $n_x h + n_y k + n_z l$ is evidently an integer, Laue's reflection condition described by (A.3) [p.20], (A.5) [p.21] and (A.6) [p.21], is satisfied when the reciprocal lattice node H_{hkl} is on the surface of Ewald sphere. Therefore, Ewald's reflection condition is equivalent to Laue's reflection condition. Furthermore, Ewald's reflection condition is also equivalent to Bragg's reflection conditions, which is more clarified by the description in the next section A.3.2

Bragg's reflection condition can easily be understood by referring to Fig. A.1 [p.20]. Laue's reflection condition is more difficult than Bragg's reflection condition. However, it can also be understood by referring to Fig. A.2 [p.21]. The drawing of Fig. A.3 in reciprocal space was invented by Ewald. This way of drawing is extremely effective when considering various difficult problems in crystallography that cannot be understood by drawing figures as shown in Fig. A.1 [p.20] and /or Fig. A.2 [p.21] in real space. It is strongly recommended to use the Ewald construction by using Fig. A.3 by paying respect to Ewald (Paul Peter Ewald, 1888/1/23~1985/8/22).

A.3.2 Relation between reciprocal lattice vector and Bragg reflection plane

Reciprocal lattice vector is a vector whose direction is perpendicular to the Bragg plane and length is $1/d'$, where d' is the lattice spacing of the Bragg plane. These are verified in the following paragraphs.

By considering $n_0 = n_x h + n_y k + n_z l$, (A.10) and (A.12)=(A.13), the following equation is obtained.

$$\overrightarrow{\text{OH}}_{hkl} \cdot (n_x\mathbf{a} + n_y\mathbf{b} + n_z\mathbf{c}) = n_0. \quad (\text{A.14})$$

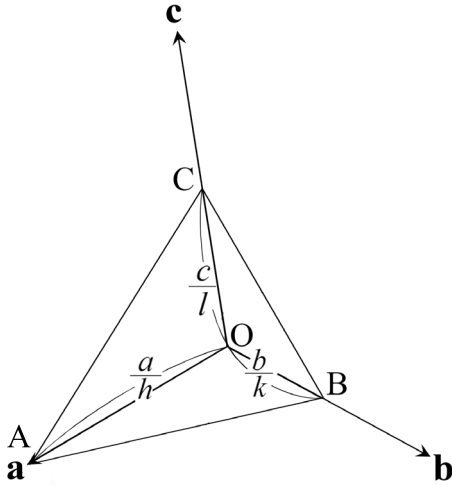


Figure A.4: Drawing of Miller and Miller indices

By multiplying $1/|\overrightarrow{OH_{hkl}}|$ to the both sides of the above equation, the following equation is obtained,

$$\frac{\overrightarrow{OH_{hkl}}}{|\overrightarrow{OH_{hkl}}|} \cdot (n_x \mathbf{a} + n_y \mathbf{b} + n_z \mathbf{c}) = \frac{n_0}{|\overrightarrow{OH_{hkl}}|}. \quad (\text{A.15})$$

A plane is described in general as follows:

$$\begin{aligned} & [\text{Unit normal vector}] \cdot [\text{Location vector}] \\ & = [\text{Distance from the origin}]. \end{aligned} \quad (\text{A.16})$$

Therefore, $n_0 \in \{\dots, -2, -1, 0, 1, 2, \dots\}$ in (A.15) means that location vector $n_x \mathbf{a} + n_y \mathbf{b} + n_z \mathbf{c}$ is on Bragg planes piled up with a spacing of $d' (= 1/|\overrightarrow{OH_{hkl}}|)$, which reveals that the reciprocal lattice vector $\overrightarrow{OH_{hkl}}$ is the normal vector of Bragg plane whose length is $1/d'$.

A.4 Drawing of Miller and Miller indices

Fig. A.4 shows the relation between the Miller indices and the Bragg plane and is found in almost all text books describing the crystallography. This way of drawing was invented by Miller (William Hallows Miller; 1801/4/6-1880/5/20). However, it should be noted that

he was a mineralogist of the 19th century before X-rays and X-ray diffraction were invented. Figs. A.1[p.20] and A.4 are found in many text books. However, it cannot be recommended that the students and researchers attempt to understand the X-ray diffraction phenomena only by referring to Figs. A.1[p.20] and A.4.

Points A, B and C in Fig. A.4 exist on \mathbf{a} , \mathbf{b} and \mathbf{c} axes, respectively. Distances of them from the origin O are a/h , b/k and c/l . Miller invented that \mathbf{a} , \mathbf{b} and \mathbf{c} axes can be defined such that all facets of crystals are drawn as shown in Fig. A.4 with small integers h , k and l .

When $h = 0$, distance of A from O is infinite and then the plane ABC is parallel to \mathbf{a} . This is the case for k , B and \mathbf{b} and for l , C and \mathbf{c} .

h , k and l are indices of reciprocal lattice nodes, which was clarified several decades after Miller's invention. ABC is a plane whose direction is parallel to the Bragg plane and distance from O is d' . These are confirmed in the following description.

By referring to Fig. A.4, $\overrightarrow{AB} = -\mathbf{a}/h + \mathbf{b}/k$ and then $\overrightarrow{AB} \cdot \overrightarrow{OH_{hkl}}$ is calculated as follows:

$$\begin{aligned} \overrightarrow{AB} \cdot \overrightarrow{OH_{hkl}} &= (-\mathbf{a}/h + \mathbf{b}/k) \cdot (h\mathbf{a}^* + k\mathbf{b}^* + l\mathbf{c}^*) \\ &= -1 + 1 \\ &= 0. \end{aligned} \quad (\text{A.17})$$

Therefore, line AB is confirmed to be perpendicular to $\overrightarrow{OH_{hkl}}$. Similarly, lines BC and CA are confirmed to be perpendicular to $\overrightarrow{OH_{hkl}}$. Further, from this, the distance of ABC from the origin O can be obtained from scalar product between the unit normal vector of plane ABC and vector \overrightarrow{OA} , \overrightarrow{OB} or \overrightarrow{OC} as follows:

$$\begin{aligned} & \overrightarrow{OA} \cdot \overrightarrow{OH_{hkl}} / |\overrightarrow{OH_{hkl}}| \\ &= \frac{\mathbf{a}}{h} (h\mathbf{a}^* + k\mathbf{b}^* + l\mathbf{c}^*) / |\overrightarrow{OH_{hkl}}| \\ &= 1 / |\overrightarrow{OH_{hkl}}| \\ &= d' \end{aligned} \quad (\text{A.18})$$

As described above, the explanation of Fig. A.4 needs complex descriptions. It cannot be recommended to understand the phenomena of X-ray diffraction only referring to the drawing of Miller as shown in Fig. A.4.

Appendix B

Determination of space group from extinction rule

==> general reflections sorted into even/odd parity classes

eee			eoo			ooo		
totl	obsd	<I/sig>	totl	obsd	<I/sig>	totl	obsd	<I/sig>
205	196	30.0	253	240	29.2	289	272	32.1
eoo			ooo			ooo		
370	354	38.4	337	322	40.5	419	392	40.3
ooo			ooo			ooo		
318	297	33.6	355	343	38.6			

==> Special reflections sorted into various classes
 A * indicates a potential systematic absence and is used if the average I/sig(I) for a particular class is less than 3.5.

ee			eo		
totl	obsd	<I/sig>	totl	obsd	<I/sig>
hhf refl	27	24	48.5	36	35
h-hf refl	30	28	49.2	37	35
Okf zone	89	80	43.2	110	106
h0f zone	34	31	43.8	40	11
hk0 zone	62	57	39.1	68	65

oe			oo		
totl	obsd	<I/sig>	totl	obsd	<I/sig>
hhf refl	40	39	45.4	47	44
h-hf refl	40	38	48.0	44	40
Okf zone	97	94	53.9	109	103
h0f zone	36	36	73.1	43	13
hk0 zone	71	64	46.7	74	72

e			o			
totl	obsd	<I/sig>	totl	obsd	<I/sig>	% of o/e
hhh line	2	2	31.3	7	5	71.6
hh0 zone	7	7	42.2	9	9	98.6
Ok0 line	17	17	74.6	16	2	1.7*
00f line	10	8	102.3	9	1	2.4*
h00 line	3	3	95.0	6	6	38.3

Figure B.1: Content of 'process.out' (#1). [Taurine; monoclinic $P2_1/c$ (#14)].

One of the most important process in the crystal structure analysis is determination of space group. CrystalStructure 4.1 determines the space group automatically as shown in Fig. B.3.

In this chapter, how the computer determines the space group, is described. When the computer failed to determine the space group correctly, it should be determined manually referring to the description of this chapter.

Figs. B.1, B.2 and B.3 show contents of 'process.out' displayed by clicking 'View output file' button in Fig. 2.12 of Part2a manual. In this file, information about the extinction rule based

==> reflections sorted for identifying 4n type conditions
 a and b represent h, k, or l

a+b=4n			a+b not equal 4n		
totl	obsd	<I/sig>	totl	obsd	<I/sig>
Okf zone	106	102	49.6	299	281
h0f zone	37	20	18.2	116	71
hk0 zone	69	66	38.9	206	192

a=4n			a not equal 4n		
totl	obsd	<I/sig>	totl	obsd	<I/sig>
Ok0 line	8	8	77.5	25	11
00f zone	4	2	60.2	15	7
h00 zone	1	1	91.3	8	8

2h+l=4n			2h+l not equal 4n		
totl	obsd	<I/sig>	totl	obsd	<I/sig>
hhf refl	34	32	47.5	116	110

==> reflections sorted for identifying 3n and 6n type conditions

h+l=3n; l odd			h+l=3n			h+l not equal 3n		
totl	obsd	<I/sig>	totl	obsd	<I/sig>	totl	obsd	<I/sig>
h-h0f	26	24	54.1	54	52	97	89	51.8

-h+l=3n; l even			-h+l=3n			-h+l not equal 3n		
totl	obsd	<I/sig>	totl	obsd	<I/sig>	totl	obsd	<I/sig>
h-h0f	26	22	62.7	49	43	102	98	56.7

l=3n			l not equal 3n		
totl	obsd	<I/sig>	totl	obsd	<I/sig>
000f line	7	2	32.5	12	7

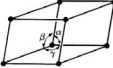
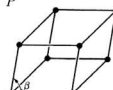

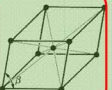
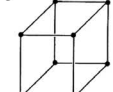



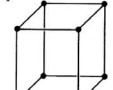
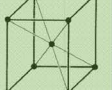
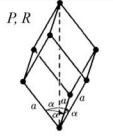
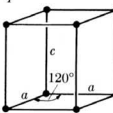
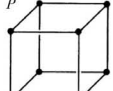


l=6n			l not equal 6n		
totl	obsd	<I/sig>	totl	obsd	<I/sig>
000f line	2	2	185.7	17	7

Figure B.2: Content of 'process.out' (#2). [Taurine; monoclinic $P2_1/c$ (#14)]

on which the space group can be determined, are summarized.

Information about extinctions of reflections whose three, two or one indices are not zero, are summarized on parts [1], [2, 3] and [4], respectively, of Fig. B.1. For example, 'eoo' found on the upper part of [1] in Fig. B.1 means that indices of hkl are even, even and odd. 'totl' and 'obsd' are numbers of total and observed reflections. $\langle I/\sigma \rangle$ are mean values of I/σ , where I is observed intensity of reflected X-rays and σ is standard deviation of background. Since values of 'obsd' and $\langle I/\sigma \rangle$ are sufficiently large, there is no extinction for three nonzero hkl . On parts [2] and [3] in Fig. B.1, $h0l$ reflections are

Table B.1: 14 Bravais lattices and ‘Face-centered monoclinic’. Refer to the last paragraph of §B.2 [p.27], please about why ‘Face-centered monoclinic’ is added.

Crystal system Laue group (No. of space group)	Axial distances (a, b, c) Axial angles (α, β, γ)	Primitive lattice (P, R)	Base-centered lattice (A, B, C)	Body-centered lattice (I)	Face-centered lattice (F)
Triclinic $\bar{1}$ (#1, #2)	$a \neq b \neq c$ $\alpha \neq \beta \neq \gamma$	P 			
Monoclinic $2/m$ (#3 ~#15)	$a \neq b \neq c$ two of α, β, γ $= 90^\circ$, one $\neq 90^\circ$	P 			
Orthorhombic mmm (#16 ~#74)	$a \neq b \neq c$ $\alpha = \beta = \gamma$ $= 90^\circ$	P 			
Tetragonal $4/m$ (#75 ~#88), $4/mmm$ (#89 ~#142)	Two of a, b, c are the same. One of them is different. $\alpha = \beta = \gamma$ $= 90^\circ$	P 			
Trigonal $\bar{3}$ (#143 ~#148), $\bar{3}m$ (#149 ~#167)	$a = b = c$ $\alpha = \beta = \gamma$ $\neq 90^\circ$	P, R 			
Hexagonal $6/m$ (#168 ~#176) $6/mmm$ (#177 ~#194)	a and b are the same. c is different. $\alpha = \beta = 90^\circ$ $\gamma = 120^\circ$	P 			
Cubic $m\bar{3}$ (#195 ~#206) $m\bar{3}m$ (#207 ~#230)	$a = b = c$, $\alpha = \beta = \gamma$ $= 90^\circ$	P 			

Space group # 14 setting # 1
The selected space group symbol is: $P2_1/c$

Figure B.3: Content of ‘process.out’ (#3) [Taurine; monoclinic $P2_1/c$ (#14)]. [setting #1] corresponds to ‘[1] CELL CHOICE 1’ in Fig. B.5.

recognized to distinguish since value of $\langle I/\text{sig} \rangle$ is extremely small when l is odd. This is indicated by an ‘*’ mark. Similarly, in part [4] in Fig. B.1, $0k0$ and $00l$ reflections are recognized to distinguish when k is odd and l is odd, respectively since values of $\langle I/\text{sig} \rangle$ and ‘% of o/e ’ are extremely small. In parts [5] and [6] in

Reflection conditions

General:

$$h0l : l = 2n$$

$$0k0 : k = 2n$$

$$00l : l = 2n$$

Figure B.4: Reflection condition of $P2_1/c$ (#14) described in *International Tables for Crystallography* (2006) Vol.A. $0k0$ reflections when k is odd and, $h0l$ and $00l$ reflections when l is odd, extinguish.

Fig. B.2, information about reflection indices when indices or summation of them are

Table B.2: Symmetric elements (planes). Protein crystals do not have these symmetric elements absolutely.

Name of symmetric plane	Symbol	Graphic symbol (perpendicular to the space)	Graphic symbol (parallel to the space)
Mirror plane	m		
Axial glide plane	a, b or c	(Glide parallel to the space) 	
Axial glide plane	a, b or c	(Glide perpendicular to the space) 	
Double glide plane	e		
Diagonal glide plane	n		
Diamond glide plane	d		

divided by 4, by 3 and by 6, from which existence of four-, three- and six-fold screw axes can be discussed.

Fig. B.3 [p.25] shows that the space group of taurine crystal has been determined to be $P2_1/c(\#14)$.

Fig. B.4 shows reflection condition of $P2_1/c(\#14)$ described in *International Tables for Crystallography* (2006) Vol.A. The information described in Figs. B.1 [p.24] and B.2 [p.24] coincides with the condition in Fig. B.4 [p.25], from which the space group has been determined to be $P2_1/c(\#14)$.

In the following description, how the extinction of reflections are caused by symmetries of crystals depending on the space group, is explained.

B.1 Symmetric elements of crystal derived based on the group theory

Who showed the importance of group theory to determine the crystal structure for the first time was Shoji Nishikawa (1884/12/5~1952/1/5). Wyckoff (R. W. G. Wyckoff; 1897/8/9~1994/11/3)

Table B.3: Symmetric elements of crystal (axes and point).

Symmetric axis or center	Symbol	Graphic symbol (perpendicular to the space)	Graphic symbol (parallel to the space)
-	1		
Two-fold rotation axis	2		
2_1 screw axis	2_1		
Three-fold rotation axis	3		
3_1 screw axis	3_1		
3_2 screw axis	3_2		
Four-fold rotation axis	4		
4_1 screw axis	4_1		
4_2 screw axis	4_2		
4_3 screw axis	4_3		
Six-fold rotation axis	6		
6_1 screw axis	6_1		
6_2 screw axis	6_2		
6_3 screw axis	6_3		
6_4 screw axis	6_4		
6_5 screw axis	6_5		
Symmetry center	$\bar{1}$		
Three-fold rotatory inversion axis	$\bar{3}$		
Four-fold rotatory inversion axis	$\bar{4}$		
Six-fold rotatory inversion axis	$\bar{6}$		

who was strongly influenced by Nishikawa, systemized and established the space group theory that is widespread today and summarized in *International Tables for Crystallography* (2006) Vol.A.

As shown in Table B.1 [p.25], crystals are categorized into seven crystal systems depending on their shapes of unit cells. Further, there are several complex lattices whose backgrounds in Table B.1 [p.25] are green, other than primitive cells. Fourteen kinds of lattice except for ‘body-centered monoclinic lattice’ are called Bravais lattice.

‘Body-centered monoclinic lattice’ was added by the present author’s own judgment. The reason is that base-centered monoclinic lattice can sometimes change to body-centered lattice without changing the symmetry of monoclinic lattice or changing volume of unit cell by reselecting axes of unit cell.

In the first column of Table B.1 [p.25], Laue groups and ranges of space group number are summarized. Laue group is determined by symmetry of reciprocal lattice of crystals.

It has been clarified that crystals can be categorized into 230 space groups depending on the symmetric elements as shown in Tables. B.1 [p.25], B.2 and B.3.

What is important to determine the space group is the extinction rule, about which the

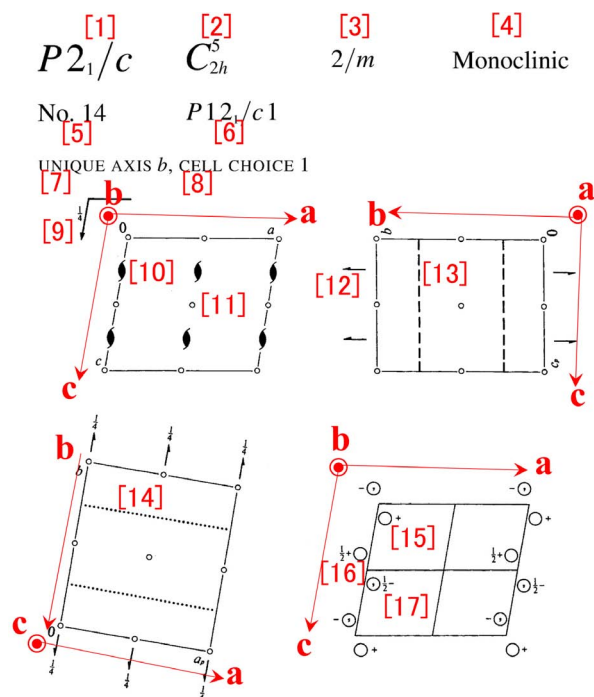


Figure B.5: Drawings for space group $P2_1/c$ (#14) in *International Tables for Crystallography* (2006) Vol.A. Protein crystals do not belong to this space group absolutely.

information can be extracted by referring to descriptions in ‘process.out’ as shown in Figs. B.1 [p.24] and B.2 [p.24]. It can be viewed by clicking ‘View output file’ button in Fig. 2.21 of Part 2a manual.

B.2 Symbols of space groups

Fig. B.5 is a diagram on the first two pages showing symmetric elements of crystal group $P12_1/c1$ in *International Tables for Crystallography* (2006) Vol.A, Chapter 7. Marks [1]-[17] are as follows; [1]: Hermann-Mouguin notation, [2]: Schönflies notation, [3]: Laue group, [4]: crystal system, [5]: ordinal number of space group, [6]: Hermann-Mouguin full notation, [7]: unique axis, [8]: cell choice, [9]: graphic symbol of c glide plane, [10]: graphic symbol of 2_1 screw axis, [11]: graphic symbol of symmetric center, [12]: graphic symbol of 2_1 screw axis, [13]: graphic symbol of c glide plane, [14]: graphic symbol of c glide plane, [15]: position of atom, [16]: position of atom (an image due to 2_1 screw axis), [17]: position of atom (an image

Table B.4: Extinctions owing to complex lattice.

Name of lattice	Symbol	Reflection condition(not extinct)	Example
A base-centered	A	$hkl : k + l = 2n$	$A12/n1$ (#15)
B base-centered	B	$hkl : h + l = 2n$	$B2/n11$ (#15)
C base-centered	C	$hkl : h + k = 2n$	$C12/c1$ (#15)
Body-centered	I	$hkl : h + k + l = 2n$	$I2/b11$ (#15)
Face-centered	F	$hkl : h + k, h + l, k + l = 2n$	

Table B.5: Extinction rules owing to glide planes. Protein crystals do not have glide plane absolutely.

Name of glide plane (Symbol)	Normal to	Reflection condition (not extinct)	Example
Axial glide plane (a)	b	$h0l : h = 2n$	$P12_1/a1$ (#14)
Axial glide plane (a)	c	$hk0 : h = 2n$	$P112_1/a$ (#14)
Axial glide plane (b)	a	$0kl : k = 2n$	$P2_1/b11$ (#14)
Axial glide plane (b)	c	$hk0 : k = 2n$	$P112_1/b$ (#14)
Axial glide plane (c)	a	$0kl : l = 2n$	$P2_1/c11$ (#14)
Axial glide plane (c)	b	$h0l : l = 2n$	$P12_1/c1$ (#14) $C12/c1$ (#15)
Double glide plane (e)	a	$hkl : k + l = 2n$	
Double glide plane (e)	b	$hkl : h + l = 2n$	
Double glide plane (e)	c	$hkl : h + k = 2n$	
Diagonal glide plane (n)	a	$0kl : k + l = 2n$	$B2/n11$ (#15)
Diagonal glide plane (n)	b	$h0l : h + l = 2n$	$C12/c1$ (#15)
Diagonal glide plane (n)	c	$hk0 : h + k = 2n$	$P112_1/n$ (#14)

due to c glide plane).

‘[8] CELL CHOICE 1’ corresponds to ‘setting #1’ in Fig. B.3 [p.25]. ‘ $\frac{1}{4}$ ’ described near [9] is the height of c glide plane. About graphic symbols of c glide plane [9], [13] and [14], refer to Table B.2 [p.26], please. About graphic symbols of 2_1 screw axis [10] and [12], refer to Table B.3 [p.26]. Atoms at positions [16] and [17] are images of atom at [15] by symmetric operations due to 2_1 screw axis and c glide plane, respectively. ‘ $\frac{1}{2}+$ ’ near [16] and ‘ $\frac{1}{2}-$ ’ near [17] means that locations of atoms at [16] and [17] are $-x\mathbf{a} + (\frac{1}{2} + y)\mathbf{b} + (\frac{1}{2} - z)\mathbf{c}$ and $x\mathbf{a} + (\frac{1}{2} - y)\mathbf{b} + (\frac{1}{2} + z)\mathbf{c}$, respectively when that of [15] is $x\mathbf{a} + y\mathbf{b} + z\mathbf{c}$. Comma (,) in ‘ \bigcirc ’ at [17] means that this atom (or molecule) is an enantiomer of those at [15] and [16].

Initial character of Hermann-Mouguin notation is P (or R partially for trigonal system) for primitive lattice, A , B or C for base-centered lattice, I for body-centered lattice or F for face-centered lattice. In many cases of base-centered lattice, C is mainly used for H-M notations. However, there are four exceptions,

Table B.6: Extinction owing to screw axes.

Name of screw axis	Direction	Reflection condition (not extinct)	Example
2 ₁ screw axis	a	$h00: h = 2n$	$P2_12_1$ (#19)
2 ₁ screw axis	b	$0k0: k = 2n$	$P12_1$ (#4)
			$P12_1/c1$ (#14)
			$C12/c1$ (#15)
			$P2_12_1$ (#19)
2 ₁ screw axis	c	$00l: l = 2n$	$P2_12_1$ (#19)
3 ₁ screw axis	c	$00l: l = 3n$	
3 ₂ screw axis	c	$00l: l = 3n$	
4 ₁ screw axis	c	$00l: l = 4n$	
4 ₂ screw axis	c	$00l: l = 2n$	
4 ₃ screw axis	c	$00l: l = 4n$	
6 ₁ screw axis	c	$00l: l = 6n$	
6 ₂ screw axis	c	$00l: l = 3n$	
6 ₃ screw axis	c	$00l: l = 2n$	
6 ₄ screw axis	c	$00l: l = 3n$	
6 ₅ screw axis	c	$00l: l = 6n$	

i.e. $Amm2$ (#38), $Abm2$ (#39), $Ama2$ (#40) and $Aba2$ (#41).

There are nine H-M full notations, i.e. $P12_1/c1$, $P12_1/n1$, $P12_1/a1$, $P112_1/a$, $P112_1/n$, $P112_1/b$, $P2_1/b11$, $P2_1/n11$, $P2_1/c11$ for $P2_1/c$ due to arbitrariness to take axes. There are plural H-M full notations for an H-M notation in general. In some cases, however, there is only one H-M full notation, e.g. $P2_12_12_1$ (orthorhombic #19) since it has an identical symmetric element all in the directions of a , b and c axes.

In the case of $C2/c$, one of H-M full notation is $I12/a1$ when changing the choice of unit cell axes. This is the reason for ‘body-centered monoclinic lattice’ is added in Table B.1 [p.25].

B.3 How to read extinction rules

In this section, how to determine the space group by reading ‘process.out’ as shown in Figs. B.1 [p.24] and B.2 [p.24] and comparing them with *International Tables for Crystallography* (2006) Vol.A, Chapter 3.1, is described. When the space group were determined not correctly, it should be redetermined referring to the following description.

Table B.7 shows a part of *International Ta-*

Table B.7: *International Tables for Crystallography* (2006) Vol.A, A part of *International Tables for Crystallography* (2006) Vol.A, Chapter 3.1.

MONOCLINIC, Laue class $2/m$

Unique axis b				Laue class $1\ 2/m\ 1$		
Reflection condition				Point group		
hkl	$h0l$	$0k0$	Extinction symbol	2	m	$2/m$
$Ok\ l\ hk0$	$h00\ 00l$	$0k0$	$P1-1$	$P121$ (3)	$P1m1$ (6)	$P1\ 2/m\ 1$ (10)
		k	$P12_11$	$P121$ (4)		$P1\ 2_1/m\ 1$ (11)
			$P1a1$		$P1a1$ (7)	$P1\ 2/a\ 1$ (13)
[1] h	k		$P1\ 2_1/a\ 1$			$P1\ 2_1/a\ 1$ (14)
[2] l			$P1c1$		$P1c1$ (7)	$P1\ 2/c\ 1$ (13)
[3] $h+l$	k		$P1\ 2_1/c\ 1$			$P1\ 2_1/c\ 1$ (14)
	$h+l$		$P1n1$		$P1n1$ (7)	$P1\ 2/n\ 1$ (13)
	$h+l$	k	$P1\ 2_1/n\ 1$			$P1\ 2_1/n\ 1$ (14)
$h+k$	h	k	$C1-1$	$C121$ (5)	$C1m1$ (8)	$C1\ 2/m\ 1$ (12)
$h+k$	h, l	k	$C1c1$		$C1c1$ (9)	$C1\ 2/c\ 1$ (15)
$k+l$	l	k	$A1-1$	$A121$ (5)	$A1m1$ (8)	$A1\ 2/m\ 1$ (12)
$k+l$	h, l	k	$A1n1$		$A1n1$ (9)	$A1\ 2/n\ 1$ (15)
$h+k+l$	$h+l$	k	$I1-1$	$I121$ (5)	$I1m1$ (8)	$I1\ 2/m\ 1$ (12)
$h+k+l$	h, l	k	$I1a1$		$I1a1$ (9)	$I1\ 2/a\ 1$ (15)

bles for Crystallography (2006) Vol.A, Chapter 3.1. Here, relations between the extinction rule and space group, are summarized. You can refer to pdf version of *International Tables for Crystallography* (2006) Vol.A, Chapter 3.1 that is placed on the desktop of computers.

In part [1] of Fig. B.1 [p.24] reflection conditions for hkl all of which are not zero, is described. Since no extinction can be found, the first column of Table B.7 should be empty. $h+k$, $k+l$ and $h+k+l$ in this column means that reflection indices that satisfies $h+k = 2n$, $k+l = 2n$ and $h+k+l = 2n$ do not distinguish. In first, second and third column in Table B.7, ‘= 2n’ is omitted.

In the case of Fig. B.1 [p.24], $0k0$ and $00l$ reflections distinguish when k is odd and when l is odd, respectively, which corresponds to [1], [2] and [3] rows in Table B.7. Therefore, H-M full notation of the space group of taurine is $P12_1/a1$, $P12_1/c1$ or $P12_1/n1$. These all belong to $P2_1/c$ (#14).

For redesignating space group in Crystal-Structure 4.1, ‘Space Group’ Menu window as shown in Fig. B.6 [p.29] can be opened by clicking ‘Space Group’ from ‘Parameters’ menu. Since b axis is usually taken as the main axis in the case of monoclinic crystal system, $P12_1/c1$ should be selected. Then, click ‘Apply’ and ‘OK’ in this order, please.

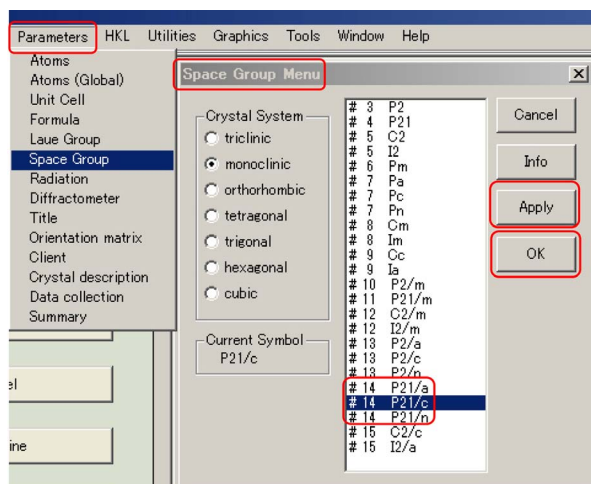


Figure B.6: Redesignation of space group in CrystalStructure 4.1. (in the case of small molecular-weight crystal).

B.4 Examples of extinction rules due to combinations of symmetric elements

In this section, several examples are described, in which the extinction rules are given by combinations of symmetric elements as summarized in Tables B.4 [p.27], B.5 [p.27] and B.6.

In cases of small molecular-weight organic crystals, frequently found space groups can be listed up in order of decreasing as follows, $P2_1/c$ (#14), $P\bar{1}$ (#2), $C2/c$ (#15), $P2_12_12_1$ (#19), $P2_1$ (#4). As many as 80% of small molecular weight organic crystals are occupied by those with space groups that belong to the above five.

In the cases of protein crystals, however, Hermann-Morguin notations of their space group do not have symbols of $\bar{1}$ (symmetric center), m (mirror plane), a , b , c , d , e and n (glide planes) absolutely since they need both optical enantiomer molecules in spite that protein molecules consist of only L amino acids but not of D amino acids. (L and D amino acids are optical enantiomer with each other). Also in the cases of small molecular-weight crystals, when they consist of chiral

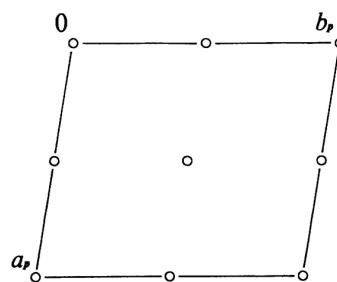


Figure B.7: Drawing for $P\bar{1}$ (#2) in *International Tables for Crystallography* (2006) Vol.A. Since this space group has symmetric center, protein crystals do not belong to it. The phase problem is simple (0 or π (180°)).

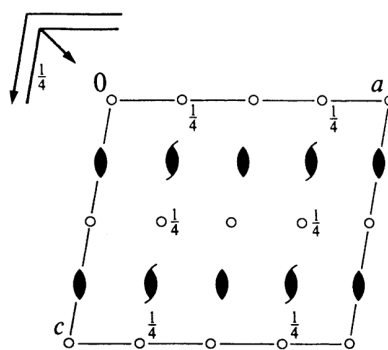


Figure B.8: Drawing for $C12/c1[C2/c]$ (#15) in *International Tables for Crystallography* (2006) Vol.A. Protein crystals do not belong to this space group absolutely since it has glide plane.

molecules, H-M notations of them do not have $\bar{1}$, m , a , b , c , d , e and n . In the cases of racemic crystals, these symbols are frequently included in their H-M notations.

Read the following description, please by referring Tables B.4 [p.27], B.5 [p.27] and B.6.

It can be read from Fig. B.5 [p.27] that space group $P2_1/c$ ($P12_1/c1$) has c glide plane and 2_1 screw axis in the direction of b . Reflection conditions due to these symmetric elements can be read from Tables B.5 [p.27] and B.6.

Reflection conditions are described in *International Tables for Crystallography* (2006) Vol.A dividing three cases in which one, two and three indices of hkl are not zero. Following this rule, the reflection conditions due to

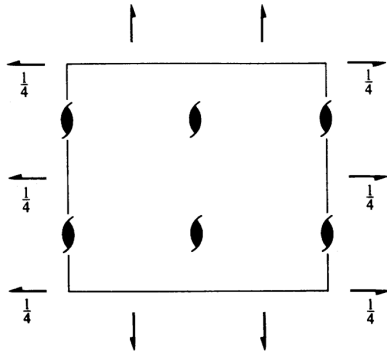


Figure B.9: *International Tables for Crystallography* (2006) Vol.A $P2_12_12_1$ (#19).

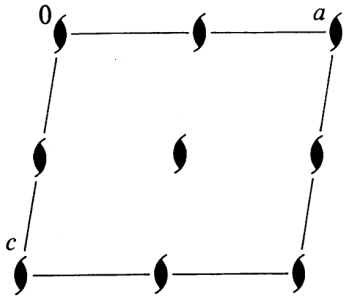


Figure B.10: *International Tables for Crystallography* (2006) Vol.A $P12_11[P2_1$ (#4)].

c glide plane and 2_1 screw axis are described as follows,

$$\begin{aligned} h0l : & \quad l = 2n, \\ 0k0 : & \quad k = 2n, \\ 00l : & \quad l = 2n. \end{aligned}$$

This is found as shown in Fig. B.4 [p.25] in *International Tables for Crystallography* (2006) Vol.A.

Symmetric element that space group $P\bar{1}$ (#2) has, is only symmetric center. Therefore, there is no extinction. Protein crystals and chiral crystals do not belong to this space group, absolutely.

However, the phase problem is extremely simple (0 or π (180°)). Therefore, the molecular structure can be obtained frequently even for a crystal with low quality.

Since the initial character of $C12/c1$ is C , it is base-centered lattice. Since there are symmetric centers indicated by small open circles, the phase problem is very simple (0 or π (180°)).

Then, the molecular structure can be solved with high possibility.

Due to arbitrariness to take axes, there are three kinds of base-centered lattice, i.e. A base-centered, B base-centered and C base-centered lattice. However, let us focus the discussion on C base-centered lattice, here. The reflection condition shown in Table B.4 [p.27] can be written down dividing it into three cases in which one, two and three indices are not zero, as follows, $[hkl : h + k = 2n]$, $[hk0 : h + k = 2n]$, $[h0l : h = 2n]$, $[0kl : k = 2n]$, $[h00 : h = 2n]$, $[0k0 : k = 2n]$.

Referring to Fig. B.8[p.29], we can understand the existence of c glide plane, n glide plane and 2_1 screw axis that are perpendicular to \mathbf{b} axis. The reflection condition due to c glide plane and n glide plane perpendicular to b axis can be read to be $[h0l : h, l = 2n]$. Further, that due to 2_1 screw axis can be read to be $[0k0 : k = 2n]$.

The logical product of the above conditions can be written down as follows,

$$\begin{aligned} hkl : & \quad h + k = 2n, \\ h0l : & \quad h, l = 2n, \\ 0kl : & \quad k = 2n, \\ hk0 : & \quad h + k = 2n, \\ 0k0 : & \quad k = 2n, \\ h00 : & \quad h = 2n, \\ 00l : & \quad l = 2n. \end{aligned}$$

B.4.1 Orthorhombic $P2_12_12_1$ (#19)

It is evident from Fig. B.9 that $P2_12_12_1$ (#19) has 2_1 screw axes all in the directions of a , b and c axes. Therefore, referring to Table B.6 [p.28], the reflection condition is given as follows,

$$\begin{aligned} h00 : & \quad h = 2n, \\ 0k0 : & \quad k = 2n, \\ 00l : & \quad l = 2n. \end{aligned}$$

B.4.2 Monoclinic $P12_11[P2_1$ (#4)]

There are three H-M full notations for space group $P2_1$ (#4). Here, the description is given for $P12_11$.

Space group $P12_11$ has 2_1 screw axis as shown in Fig. B.10. Therefore, as described in Table

B.6 [p.28], it has a reflection condition as follows,

$$0k0 : k = 2n.$$

B.5 Mathematical proofs of extinction rules

When the reader has time, refer to this chapter, please.

The extinction of reflection is caused by the existence of complex latticeC glide plane and screw axis whose background color is green in Tables B.1[p.25], B.2[p.26] and B.3[p.26]. To the contrary, only the above three symmetric elements give the extinction. However, protein crystals do not have glide plane absolutely. In this chapter, mathematical proofs of extinction due to the above symmetric elements are described.

For later description, let us note the definition of crystal structure factor, F_{hkl} for hkl reflection given as follows,

$$\begin{aligned} F_{hkl} &= \int_{\text{cell}} \rho(\mathbf{r}) \exp[-i2\pi(\mathbf{h} \cdot \mathbf{r})] dv. \\ &= \int_{\text{cell}} \rho(\mathbf{r}) \exp[-i2\pi(hx + ky + lz)] dv. \end{aligned} \quad (\text{B.1})$$

Here, $\int_{\text{cell}} dv$ is a volume integral over a unit cell, $\rho(\mathbf{r})$ is electron density at location \mathbf{r} ($= x\mathbf{a} + y\mathbf{b} + z\mathbf{c}$), and \mathbf{h} ($= h\mathbf{a}^* + k\mathbf{b}^* + l\mathbf{c}^*$) is a reciprocal lattice vector giving $h k l$ reflection. With regard to reciprocal lattice, refer to Appendix A [p.20], please.

Symmetry element that makes N equivalent points can be described as follows,

$$\rho[T^{(i)}(\mathbf{r})] = \rho[T^{(0)}(\mathbf{r})], \quad i \in \{0, 1, \dots, N-1\}.$$

Since F_{hkl} is zero when the N integral elements,

$$\sum_{i=0}^{N-1} \rho[T^{(0)}(\mathbf{r})] \exp[-i2\pi\mathbf{h} \cdot T^{(i)}(\mathbf{r})] = 0$$

That is to say,

$$\sum_{i=0}^{N-1} \exp[-i2\pi\mathbf{h} \cdot T^{(i)}(\mathbf{r})] = 0 \quad (\text{B.2})$$

B.5.1 Extinction rules due to complex lattice

Table B.4 [p.27] summarizes the extinction rules due to complex lattice. In the following description, mathematical proofs for those due to base-centered, body-centered and face-centered lattice are given.

B.5.1.1 Extinction due to base-centered lattice

Symmetry of C base-centered lattice is described as follows,

$$\begin{aligned} \rho[T_C^{(i)}(\mathbf{r})] &= \rho[T_C^{(0)}(\mathbf{r})], \quad i \in \{0, 1\}. \\ T_C^{(0)}(\mathbf{r}) &= x\mathbf{a} + y\mathbf{b} + z\mathbf{c}, \\ T_C^{(1)}(\mathbf{r}) &= (x + \frac{1}{2})\mathbf{a} + (y + \frac{1}{2})\mathbf{b} + z\mathbf{c}. \end{aligned}$$

The extinction condition is described similarly to (B.2) as follows:

$$\sum_{i=0}^1 \exp[-i2\pi\mathbf{h} \cdot T_C^{(i)}(\mathbf{r})] = 0. \quad (\text{B.3})$$

Here, mathematical convenience to calculate \sum in (B.3), let us define $f_C(\mathbf{h}, \mathbf{r})$ as follows,

$$\begin{aligned} f_C(\mathbf{h}, \mathbf{r}) &= \exp\{-i2\pi[h(x + \frac{1}{4}) + k(y + \frac{1}{4}) + lz]\}. \end{aligned}$$

Therefore, the extinction condition is described as follows,

$$\begin{aligned} f_C(\mathbf{h}, \mathbf{r}) &\times \{\exp[-i\frac{\pi}{2}(h+k)] + \exp[+i\frac{\pi}{2}(h+k)]\} \\ &= 2f_C(\mathbf{h}, \mathbf{r}) \cos[\frac{\pi}{2}(h+k)] = 0. \end{aligned}$$

Since $f_C(\mathbf{h}, \mathbf{r})$ is not zero in general, the extinction condition is given by

$$\cos[\frac{\pi}{2}(h+k)] = 0.$$

Since the above equation is satisfied when $h+k$ is odd, the reflection condition (not extinct) as shown in Table B.4 [p.27] is given by

$$hkl : @h+k = 2n$$

Here, l is an arbitrary integer.

Reflection conditions for A and B base-centered lattice can be derived similarly to the above description.

B.5.1.2 Extinction due to body-centered lattice

Symmetry of body-centered lattice is described as follows,

$$\begin{aligned}\rho[T_I^{(i)}(\mathbf{r})] &= \rho[T_I^{(0)}(\mathbf{r})], \quad i \in \{0, 1\}. \\ T_I^{(0)}(\mathbf{r}) &= x\mathbf{a} + y\mathbf{b} + z\mathbf{c}, \\ T_I^{(1)}(\mathbf{r}) &= (x + \frac{1}{2})\mathbf{a} \\ &\quad + (y + \frac{1}{2})\mathbf{b} \\ &\quad + (z + \frac{1}{2})\mathbf{c}.\end{aligned}$$

The extinction condition is described similarly to (B.2) [p.31] as follows,

$$\sum_{i=0}^1 \exp[-i2\pi\mathbf{h} \cdot T_I^{(i)}(\mathbf{r})] = 0. \quad (\text{B.4})$$

For convenience for calculation of \sum in (B.4), let $f_I(\mathbf{h}, \mathbf{r})$ be defined as follows,

$$\begin{aligned}f_I(\mathbf{h}, \mathbf{r}) &= \exp\{-i2\pi[h(x + \frac{1}{4}) \\ &\quad + k(y + \frac{1}{4}) \\ &\quad + l(z + \frac{1}{4})]\}.\end{aligned}$$

Therefore, the extinction condition is given as follows,

$$\begin{aligned}f_I(\mathbf{h}, \mathbf{r}) \times \\ \{ \exp[-i\frac{\pi}{2}(h+k+l)] \\ + \exp[+i\frac{\pi}{2}(h+k+l)] \} \\ = 2f_I(\mathbf{h}, \mathbf{r}) \cos[\frac{\pi}{2}(h+k+l)] = 0.\end{aligned}$$

Since $f_I(\mathbf{h}, \mathbf{r})$ is not zero in general, the extinction condition is given by

$$\cos[\frac{\pi}{2}(h+k+l)] = 0.$$

Since the above equation is satisfied when $h+k+l$ is odd, the reflection condition (not extinct) as shown in Table B.4 [p.27], is given as follows,

$$hkl : \quad h+k+l = 2n$$

B.5.1.3 Extinction due to face-centered lattice

Symmetry of face-centered lattice is described as follows,

$$\begin{aligned}\rho[T_F^{(i)}(\mathbf{r})] &= \rho[T_F^{(0)}(\mathbf{r})], \quad i \in \{0, 1, 2, 3\}. \\ T_F^{(0)}(\mathbf{r}) &= x\mathbf{a} + y\mathbf{b} + z\mathbf{c}, \\ T_F^{(1)}(\mathbf{r}) &= x\mathbf{a} + (y + \frac{1}{2})\mathbf{b} + (z + \frac{1}{2})\mathbf{c}, \\ T_F^{(2)}(\mathbf{r}) &= (x + \frac{1}{2})\mathbf{a} + y\mathbf{b} + (z + \frac{1}{2})\mathbf{c}, \\ T_F^{(3)}(\mathbf{r}) &= (x + \frac{1}{2})\mathbf{a} + (y + \frac{1}{2})\mathbf{b} + z\mathbf{c}.\end{aligned}$$

The extinction condition is described similarly to (B.2) [p.31] by the following equation,

$$\sum_{i=0}^3 \exp[-i2\pi\mathbf{h} \cdot T_F^{(i)}(\mathbf{r})] = 0. \quad (\text{B.5})$$

Here, for mathematical convenience to calculate \sum in (B.5), let us define $f_F(\mathbf{h}, \mathbf{r})$ as follows,

$$\begin{aligned}f_F(\mathbf{h}, \mathbf{r}) &= \exp\{-i2\pi[h(x + \frac{1}{4}) \\ &\quad + k(y + \frac{1}{4}) \\ &\quad + l(z + \frac{1}{4})]\}.\end{aligned}$$

Therefore, the extinction condition is given as follows,

$$\begin{aligned}f_F(\mathbf{h}, \mathbf{r}) \{ \exp[-i\frac{\pi}{2}(-h-k-l)] \\ + \exp[-i\frac{\pi}{2}(-h+k+l)] \\ + \exp[-i\frac{\pi}{2}(+h-k+l)] \\ + \exp[-i\frac{\pi}{2}(+h+k-l)] \} \\ = 2f_F(\mathbf{h}, \mathbf{r}) \{ \exp(+i\frac{\pi}{2}h) \cos[\frac{\pi}{2}(k+l)] \\ + \exp(-i\frac{\pi}{2}h) \cos[\frac{\pi}{2}(k-l)] \} = 0.\end{aligned} \quad (\text{B.6})$$

$$\begin{aligned} = 2f_F(\mathbf{h}, \mathbf{r}) \{ \exp(+i\frac{\pi}{2}h) \cos[\frac{\pi}{2}(k+l)] \\ + \exp(-i\frac{\pi}{2}h) \cos[\frac{\pi}{2}(k-l)] \} = 0.\end{aligned} \quad (\text{B.7})$$

Since $f_F(\mathbf{h}, \mathbf{r})$ is not zero in general, the extinction condition is represented as follows,

$$\begin{aligned}\cos[\frac{\pi}{2}(k+l)] &= 0, \\ \cos[\frac{\pi}{2}(k-l)] &= 0.\end{aligned}$$

$[(k + l \text{ is even}) \text{ and } (k - l \text{ is even})]$ is identical to $[(\text{both } k \text{ and } l \text{ are even}) \text{ or } (\text{both } k \text{ and } l \text{ are odd})]$ i.e. $k + l = 2n$. Here, h is an arbitrary integer. Since (B.6) is symmetrical for h, k and l , equations similar to (B.7) can be derived also for $h + k, h - k$ and $h + l, h - l$. Then, The reflection condition (not distinguishing) as shown in Table B.4 [p.27] is given by

$$\begin{aligned}
 hkl : \quad h + k &= 2n, \\
 hkl : \quad h + l &= 2n, \\
 hkl : \quad l + k &= 2n.
 \end{aligned}$$

That is to say, reflection distinguishes when even and odd integers are mixed in h, k and l .

B.5.2 Extinction owing to glide axes

In cases of protein crystals, they do not have glide axis absolutely since they consist of only L amino acids but of not D amino acids (optical isomers of L amino acids).

B.5.2.1 Extinction due to axial glide plane

Symmetry due to c glide plane perpendicular to \mathbf{b} axis whose height is $\frac{1}{4}\mathbf{b}$, is given by

$$\begin{aligned}
 \rho[T_{Bc}^{(i)}(\mathbf{r})] &= \rho[T_{Bc}^{(0)}(\mathbf{r})], \quad i \in \{0, 1\}. \\
 T_{Bc}^{(0)}(\mathbf{r}) &= x\mathbf{a} + y\mathbf{b} + z\mathbf{c}, \\
 T_{Bc}^{(1)}(\mathbf{r}) &= x\mathbf{a} + \left(\frac{1}{2} - y\right)\mathbf{b} + \left(\frac{1}{2} + z\right)\mathbf{c},
 \end{aligned}$$

Similarly to (B.2) [p.31], the extinction condition is given by

$$\sum_{i=0}^1 \exp[-i2\pi\mathbf{h} \cdot T_{Bc}^{(i)}(\mathbf{r})] = 0. \quad (\text{B.8})$$

Here, for mathematical convenience to calculate \sum in (B.8) [p.33], let us define $f_{Bc}(\mathbf{h}, \mathbf{r})$ as follows,

$$\begin{aligned}
 f_{Bc}(\mathbf{h}, \mathbf{r}) &= \exp\{-i2\pi[hx + k\frac{1}{4} + l(\frac{1}{4} + z)]\}. \\
 f_{Bc}(\mathbf{h}, \mathbf{r}) \times \\
 &\left\{ \exp\{+i2\pi[k(\frac{1}{4} - y) + l\frac{1}{4}]\} \right. \\
 &+ \left. \exp\{-i2\pi[k(\frac{1}{4} - y) + l\frac{1}{4}]\} \right\} \\
 &= 2f_{Bc}(\mathbf{h}, \mathbf{r}) \cos\left\{\frac{\pi}{2}[k(1 - 4y) + l]\right\} = 0.
 \end{aligned}$$

Since $f_F(\mathbf{h}, \mathbf{r})$ is not zero in general, reflections distinguish when the term of $\cos\{\}$ is zero, i.e. when h is arbitrary, $k = 0$ and l is odd, the reflection condition as shown in Table B.5 [p.27] is given by

$$h0l : \quad l = 2n$$

B.5.2.2 Extinction due to double glide plane (e glide plane)

Therefore, Symmetry due to double glide plane (e glide plane) whose height is zero, is described as follows,

$$\begin{aligned}
 \rho[T_{Be}^{(i)}(\mathbf{r})] &= \rho[T_{Be}^{(0)}(\mathbf{r})], \quad i \in \{0, 1, 2, 3\}. \\
 T_{Be}^{(0)}(\mathbf{r}) &= x\mathbf{a} + y\mathbf{b} + z\mathbf{c}, \\
 T_{Be}^{(1)}(\mathbf{r}) &= \left(x + \frac{1}{2}\right)\mathbf{a} - y\mathbf{b} + z\mathbf{c}, \\
 T_{Be}^{(2)}(\mathbf{r}) &= x\mathbf{a} - y\mathbf{b} + \left(z + \frac{1}{2}\right)\mathbf{c}, \\
 T_{Be}^{(3)}(\mathbf{r}) &= \left(x + \frac{1}{2}\right)\mathbf{a} + y\mathbf{b} + \left(z + \frac{1}{2}\right)\mathbf{c},
 \end{aligned}$$

Similarly to (B.2) [p.31], the extinction rule is described by

$$\sum_{i=0}^3 \exp[-i2\pi\mathbf{h} \cdot T_{Be}^{(i)}(\mathbf{r})] = 0. \quad (\text{B.9})$$

Here, for mathematical convenience to calculate \sum in (B.9), let us define $f_{Be}(\mathbf{h}, \mathbf{r})$ as follows,

$$f_{Be}(\mathbf{h}, \mathbf{r}) = \exp\{-i2\pi[h(\frac{1}{4} + x) + l(\frac{1}{4} + z)]\}.$$

Therefore, the extinction condition can be described as follows,

$$\begin{aligned}
 &f_{Be}(\mathbf{h}, \mathbf{r}) \times \\
 &\left\{ \exp\{-i2\pi[-h\frac{1}{4} + ky - l\frac{1}{4}]\} \right. \\
 &+ \exp\{-i2\pi[+h\frac{1}{4} - ky - l\frac{1}{4}]\} \\
 &+ \exp\{-i2\pi[-h\frac{1}{4} - ky + l\frac{1}{4}]\} \\
 &+ \left. \exp\{-i2\pi[+h\frac{1}{4} + ky + l\frac{1}{4}]\} \right\} \\
 &= 2f_{Be}(\mathbf{h}, \mathbf{r}) \times \\
 &\left\{ \exp(-i2\pi ky) \cos\left[\frac{\pi}{2}(h + l)\right] \right. \\
 &+ \left. \exp(+i2\pi ky) \cos\left[\frac{\pi}{2}(h - l)\right] \right\} = 0.
 \end{aligned}$$

Since $f_{Be}(\mathbf{h}, \mathbf{r})$ and $\exp(\pm i2\pi ky)$ are not zero in general, the above extinction condition is satisfied when $\cos[\frac{\pi}{2}(h+l)] = 0 \cos[\frac{\pi}{2}(h-l)] = 0$. hkl reflections distinguishes when both $h+l$ and $h-l$ are odd, i.e. when k is arbitrary and $[(h, k \text{ are odd}) \text{ or } (h, k \text{ are even})]$. The reflection condition (not extinct) is given by

$$hkl : h + l = 2n$$

With regard to other double glide planes, extinction rules as shown in Table B.5 [p.27] can be derived in a similar way.

B.5.2.3 Extinction due to diagonal glide plane

Symmetry due to diagonal glide plane (n glide plane) whose height is zero, is described as follows,

$$\rho[T_{Bn}^{(i)}(\mathbf{r})] = \rho[T_{Bn}^{(0)}(\mathbf{r})], \quad i \in \{0, 1\}.$$

$$T_{Bn}^{(0)}(\mathbf{r}) = x\mathbf{a} + y\mathbf{b} + z\mathbf{c},$$

$$T_{Bn}^{(1)}(\mathbf{r}) = (\frac{1}{2} + x)\mathbf{a} - y\mathbf{b} + (\frac{1}{2} + z)\mathbf{c},$$

The extinction condition is described similarly to (B.2) [p.31] as follows,

$$\sum_{i=0}^1 \exp[-i2\pi \mathbf{h} \cdot T_{Bn}^{(i)}(\mathbf{r})] = 0. \quad (\text{B.10})$$

Here, mathematical convenience to calculate \sum in (B.10), let us define $f_{Bn}(\mathbf{h}, \mathbf{r})$ as follows,

$$f_{Bn}(\mathbf{h}, \mathbf{r}) = \exp\{-i2\pi[h(\frac{1}{4} + x) + l(\frac{1}{4} + z)]\}.$$

Therefore, the extinction condition is described as follows,

$$\begin{aligned} & f_{Bn}(\mathbf{h}, \mathbf{r}) \times \\ & \left\{ \exp\{-i2\pi[-h\frac{1}{4} + ky - l\frac{1}{4}]\} \right. \\ & \left. + \exp\{-i2\pi[h\frac{1}{4} - ky + l\frac{1}{4}]\} \right\} \\ & = 2f_{Bn}(\mathbf{h}, \mathbf{r}) \cos\{\frac{\pi}{2}[4ky - (h+l)]\} = 0. \end{aligned}$$

Since $f_{Bn}(\mathbf{h}, \mathbf{r})$ is not zero in general, hkl reflections distinguish when the term of $\cos\{\}$ is zero. Therefore, the reflection condition (not extinct) is described as follows,

$$h0l : h + l = 2n$$

With regard to other orthogonal glide plane, reflection conditions as summarized in Table B.5 [p.27] can be derived.

B.5.3 Extinction due to screw axes

Table B.6 [p.28] summarizes extinction rules due to p_q screw axes. Here $p \in \{2, 3, 4, 6\}$ and $q \in \{1, \dots, p-1\}$, p_q screw axis makes p equivalent points such that they translate by $q\mathbf{c}/p$, ($q\mathbf{a}/p$ or $q\mathbf{b}/p$) when rotated by $2\pi/p$ around the axis. As summarized in Table B.6 [p.28], reflection condition $[00l : l = 2n]$ is given by 2_1 , 4_2 and 6_3 screw axes since they make layers of atoms (molecules) whose spacing is c , (a or b).

Similarly, reflection conditions $[000l : l = 3n]$ for 3_1 , 3_2 , 6_2 , 6_4 screw axes, $[00l : l = 4n]$ for 4_1 , 4_3 screw axes and $[000l : l = 6n]$ for 6_1 , 6_5 screw axes can be derived. For mathematical proof of reflection conditions for three- and six-fold screw axes, refer to Appendix C [p.37], please.

In the following description, mathematical proofs of extinction rules due to 2_1 , 4_1 and 4_2 screw axes.

B.5.3.1 Extinction due to 2_1 screw axis

Symmetry of 2_1 screw axis in the direction of \mathbf{c} located at $\frac{1}{2}\mathbf{a} + \frac{1}{2}\mathbf{b}$, is described as follows,

$$\rho[T_{2_1}^{(i)}(\mathbf{r})] = \rho[T_{2_1}^{(0)}(\mathbf{r})], \quad i \in \{0, 1\}.$$

$$T_{2_1}^{(0)}(\mathbf{r}) = (\frac{1}{2} + x)\mathbf{a} + (\frac{1}{2} + y)\mathbf{b} + z\mathbf{c},$$

$$T_{2_1}^{(1)}(\mathbf{r}) = (\frac{1}{2} - x)\mathbf{a} + (\frac{1}{2} - y)\mathbf{b} + (\frac{1}{2} + z)\mathbf{c}.$$

The extinction condition is described similarly to (B.2) [p.31] as follows,

$$\sum_{i=0}^1 \exp[-i2\pi \mathbf{h} \cdot T_{2_1}^{(i)}(\mathbf{r})] = 0. \quad (\text{B.11})$$

Here, for mathematical convenience to calculate \sum of (B.11), let us define $f_{2_1}(\mathbf{h}, \mathbf{r})$ as follows,

$$f_{2_1}(\mathbf{h}, \mathbf{r}) = \exp\{-i2\pi[h\frac{1}{2} + k\frac{1}{2} + l(\frac{1}{4} + z)]\}.$$

Therefore, summation in (B.11) can be deformed to give the following extinction condi-

tion,

$$\begin{aligned}
 & f_{2_1}(\mathbf{h}, \mathbf{r}) \times \\
 & \left\{ \exp\{-i2\pi[hx + ky - l\frac{1}{4}]\} \right. \\
 & \left. + \exp\{-i2\pi[-hx - ky + l\frac{1}{4}]\} \right\} \\
 & = f_{2_1}(\mathbf{h}, \mathbf{r}) \times \\
 & \cos\left\{\frac{\pi}{2}[4(hx + ky) - l]\right\} = 0.
 \end{aligned}$$

Since term of $\cos\{ \}$ is zero when $h, k = 0$ and l is odd, the reflection condition (not extinct) is given by

$$00l : \quad l = 2n.$$

Similarly, the reflection conditions due to \mathbf{c} and \mathbf{a} screw axes can be obtained as summarized in Table B.6 [p.28].

B.5.3.2 Extinction due to 4_1 screw axis

Symmetry due to 4_1 screw axis that is located at the origin, can be described as follows,

$$\begin{aligned}
 \rho[T_{4_1}^{(i)}(\mathbf{r})] &= \rho[T_{4_1}^{(0)}(\mathbf{r})], \quad i \in \{0, 1, 2, 3\}. \\
 T_{4_1}^{(0)}(\mathbf{r}) &= +x\mathbf{a} + y\mathbf{b} + \frac{1}{8}\mathbf{c}, \\
 T_{4_1}^{(1)}(\mathbf{r}) &= -y\mathbf{a} + x\mathbf{b} + \frac{3}{8}\mathbf{c}, \\
 T_{4_1}^{(2)}(\mathbf{r}) &= -x\mathbf{a} - y\mathbf{b} + \frac{5}{8}\mathbf{c}, \\
 T_{4_1}^{(3)}(\mathbf{r}) &= +y\mathbf{a} - x\mathbf{b} + \frac{7}{8}\mathbf{c}.
 \end{aligned}$$

Here, the extinction condition is described similarly to (B.2) [p.31] as follows,

$$\sum_{i=0}^3 \exp[-i2\pi\mathbf{h} \cdot T_{4_1}^{(i)}(\mathbf{r})] = 0. \quad (\text{B.12})$$

Here, let us define $f_{4_1}(\mathbf{h}, \mathbf{r})$ as follows,

$$f_{4_1}(\mathbf{h}, \mathbf{r}) = \exp(-i2\pi l \frac{1}{2}).$$

Therefore, summation in (B.12) can be deformed to give the following extinction condi-

tion,

$$\begin{aligned}
 & f_{4_1}(\mathbf{h}, \mathbf{r}) \times \\
 & \left\{ \exp[-i2\pi(+hx + ky - l\frac{3}{8})] \right. \\
 & + \exp[-i2\pi(-hy + kx - l\frac{1}{8})] \\
 & + \exp[-i2\pi(-hx - ky + l\frac{1}{8})] \\
 & \left. + \exp[-i2\pi(+hy - kx + l\frac{3}{8})] \right\} \\
 & = 2f_{4_1}(\mathbf{h}, \mathbf{r}) \times \\
 & \left\{ \exp(+i2\pi l \frac{1}{8}) \cos\left\{\frac{\pi}{2}[4(hx + ky) - l]\right\} \right. \\
 & \left. + \exp(-i2\pi l \frac{1}{8}) \cos\left\{\frac{\pi}{2}[4(hy - kx) + l]\right\} \right\} \\
 & = 0.
 \end{aligned}$$

When $h, k = 0$ and l is even, $\cos\{ \}$ in the first and second terms of the above equation have an identical value (1 or -1). Under an assumption that this condition is satisfied, let us discuss the condition that the above equation gives value of zero as follows,

$$\begin{aligned}
 & \exp(-i2\pi l \frac{1}{8}) + \exp(-i2\pi l \frac{1}{8}) \\
 & = 2 \cos\left(\frac{\pi}{2} \cdot \frac{l}{2}\right) = 0.
 \end{aligned}$$

The above equation means that reflections distinguish when $l/2$ is odd. Therefore, the reflection condition (not extinct) can be described as follows,

$$00l : \quad l = 4n.$$

Similarly, reflection condition due to 4_3 screw axis can be obtained.

B.5.3.3 Extinction due to 4_2 screw axis

Symmetry due to 4_2 screw axis at the origin can be describes as follows,

$$\begin{aligned}
 \rho[T_{4_2}^{(i)}(\mathbf{r})] &= \rho[T_{4_2}^{(0)}(\mathbf{r})], \quad i \in \{0, 1, 2, 3\}. \\
 T_{4_2}^{(0)}(\mathbf{r}) &= +x\mathbf{a} + y\mathbf{b} + \frac{1}{4}\mathbf{c}, \\
 T_{4_2}^{(1)}(\mathbf{r}) &= -y\mathbf{a} + x\mathbf{b} + \frac{3}{4}\mathbf{c}, \\
 T_{4_2}^{(2)}(\mathbf{r}) &= -x\mathbf{a} - y\mathbf{b} + \frac{1}{4}\mathbf{c}, \\
 T_{4_2}^{(3)}(\mathbf{r}) &= +y\mathbf{a} - x\mathbf{b} + \frac{3}{4}\mathbf{c}.
 \end{aligned}$$

A point translates by $\frac{2}{4}\mathbf{c}$ when rotating by $\frac{2\pi}{4}$ around the axis. Here, note that the heights of $T_{4_2}^{(2)}(\mathbf{r})$ and $T_{4_2}^{(3)}(\mathbf{r})$ are $\frac{5}{4}\mathbf{c}$ and $\frac{7}{4}\mathbf{c}$ which are equivalent to $\frac{1}{4}\mathbf{c}$, $\frac{3}{4}\mathbf{c}$ due to translation symmetry of unit cell.

The, the extinction condition is described similarly to (B.2) [p.31] as follows,

$$\sum_{i=0}^3 \exp[-i2\pi\mathbf{h} \cdot T_{4_2}^{(i)}] = 0. \quad (\text{B.13})$$

Here, for mathematical convenience to calculate \sum in (B.13), let $f_{4_2}(\mathbf{h}, \mathbf{r})$ be dined as follows,

$$f_{4_2}(\mathbf{h}, \mathbf{r}) = \exp[-i2\pi(l\frac{1}{2})].$$

$f_{4_2}(\mathbf{h}, \mathbf{r})$ Therefore, deforming the \sum of (B.13), the extinction condition can be obtained as follows,

$$\begin{aligned} & f_{4_2}(\mathbf{h}, \mathbf{r}) \times \\ & \left\{ \exp[-i2\pi(+hx + ky - l\frac{1}{4})] \right. \\ & + \exp[-i2\pi(-ky + hx + l\frac{1}{4})] \\ & + \exp[-i2\pi(-hx - ky - l\frac{1}{4})] \\ & \left. + \exp[-i2\pi(+kx - hy + l\frac{1}{4})] \right\} \end{aligned}$$

$$\begin{aligned} & = 2f_{4_2}(\mathbf{h}, \mathbf{r}) \times \\ & \left\{ \exp(+i2\pi l\frac{1}{4}) \cos[2\pi(hx + ky)] \right. \\ & \left. + \exp(-i2\pi l\frac{1}{4}) \cos[2\pi(kx - hy)] \right\} \\ & = 0. \end{aligned}$$

The above extinction can be discussed when the content of $\cos[]$ is zero. Under the assumption that the above condition is satisfied, the above equation can be further deformed as follows,

$$\begin{aligned} & \exp(-i2\pi l\frac{1}{4}) + \exp(+i2\pi l\frac{1}{4}) \\ & = 2\cos(\frac{\pi}{2}l) = 0. \end{aligned}$$

Therefore, the reflection condition (not extinct) can be described as follows,

$$00l : l = 2n.$$

Reflection condition due to 6_3 screw axis is the same as the above description. With regard to this, refer to §C.2.5 [p.42] in Appendix C, please.

Appendix C

Reflection indices and extinction rules in the cases of trigonal and hexagonal crystals

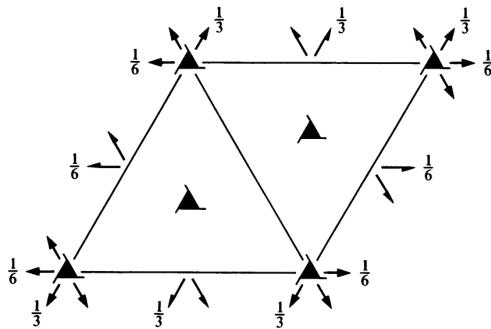


Figure C.1: *International Tables for Crystallography* (2006) Vol.A, Symmetric elements. $P3_121$ (#152).

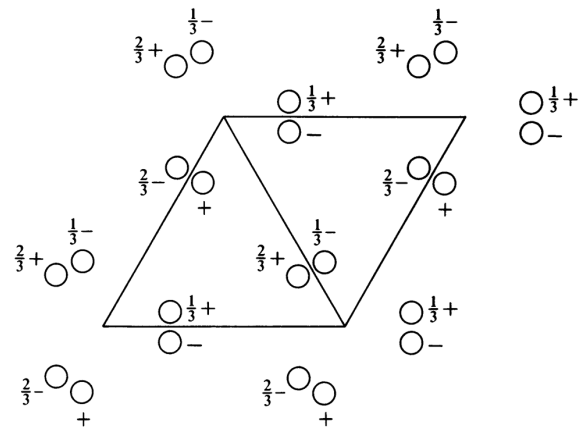


Figure C.2: *International Tables for Crystallography* (2006) Vol.A, Positions of atoms. $P3_121$ (#152).

Read this chapter when the reader has time, please.

In cases of trigonal and hexagonal crystal system, reflection vectors are usually indexed by four integers, $h k i l$ ($h + k + i = 0$). This chapter describes the reasonableness of this way of indexing and the extinction rules due to three- and six-fold screw axes.

C.1 Cases of trigonal system

C.1.1 Diagram shown in *International Tables for Crystallography* (2006) Vol.A

Fig. C.1 is a diagram in *International Tables for Crystallography* (2006) Vol.A that

shows symmetric elements of space group $P3_121$ (#152). Fig. C.2 shows atomic coordinates of $P3_121$ (#152).

The unit cell is usually taken to be a rhombus that consists of two regular triangles as shown in Figs. C.1 and C.2. Space group $P3_121$ (#152) has three-fold screw axis in the direction of \mathbf{c} axis and two-fold screw axis perpendicular to \mathbf{c} axis. However, in the case of trigonal system, there is no extinction due to the two-fold screw axis. About this, refer to the description in §C.1.4 [p.39], please.

C.1.2 Real and reciprocal coordinates

Fig. C.3 shows real and reciprocal primitive translation vectors in the cases of trigonal and hexagonal crystal system.

\mathbf{a} , \mathbf{b} and \mathbf{c} axes are usually taken such that the angle spanned by \mathbf{a} and \mathbf{b} axes is 120° and \mathbf{c} is parallel to three-fold rotation or screw axis. There are three way of taking \mathbf{a} and \mathbf{b} axes as shown in Fig. C.3 i.e. combinations of \mathbf{a}_0 and \mathbf{b}_0 axes, \mathbf{a}_1 and \mathbf{b}_1 axes and \mathbf{a}_2 and \mathbf{b}_2 axes.

reciprocal primitive vectors are defined as follows:

$$\begin{aligned}\mathbf{a}^* &= \frac{\mathbf{b} \times \mathbf{c}}{\mathbf{a} \cdot (\mathbf{b} \times \mathbf{c})}, \\ \mathbf{b}^* &= \frac{\mathbf{c} \times \mathbf{a}}{\mathbf{a} \cdot (\mathbf{b} \times \mathbf{c})}, \\ \mathbf{c}^* &= \frac{\mathbf{a} \times \mathbf{b}}{\mathbf{a} \cdot (\mathbf{b} \times \mathbf{c})}.\end{aligned}$$

About the reasonableness of the above definition, refer to Appendix A [p.20], please.

By following the above definition, in Fig. C.3, real (black) and reciprocal (gray) primitive translation vectors are drawn. Referring to this figure, the following relations can easily be understood,

$$\begin{aligned}\mathbf{a}_0^* &= -\mathbf{b}_1^* \\ &= -\mathbf{a}_2^* + \mathbf{b}_2^*, \\ \mathbf{b}_0^* &= \mathbf{a}_1^* - \mathbf{b}_1^* \\ &= -\mathbf{a}_2^*.\end{aligned}$$

From the above relations, reciprocal lattice vector $h\mathbf{a}_0^* + k\mathbf{b}_0^* + l\mathbf{c}^*$ can also be represented as follows:

$$\begin{aligned}h\mathbf{a}_0^* + k\mathbf{b}_0^* + l\mathbf{c}^* &= k\mathbf{a}_1^* + i\mathbf{b}_1^* + l\mathbf{c}^* \\ &= i\mathbf{a}_2^* + h\mathbf{b}_2^* + l\mathbf{c}^*,\end{aligned}$$

where, $h + k + i = 0$.

By using four indices h , k , i and l ($h+k+i=0$) to describe reflections, we can easily understand the equivalence of reflections due to three-fold symmetry. For example, a reflection described as $1\ 1\ 0$ by using $\mathbf{a}_0^*\text{-}\mathbf{b}_0^*\text{-}\mathbf{c}^*$ coordinate system is equivalent to $1\ \bar{2}\ 0$ by $\mathbf{a}_1^*\text{-}\mathbf{b}_1^*\text{-}\mathbf{c}^*$ system and also to $\bar{2}\ 1\ 0$ by $\mathbf{a}_2^*\text{-}\mathbf{b}_2^*\text{-}\mathbf{c}^*$ system. This reflection $1\ 1\ \bar{2}\ 0$ described using four indices can easily be understood to be equivalent to $1\ \bar{2}\ 1\ 0$ and $\bar{2}\ 1\ 1\ 0$.

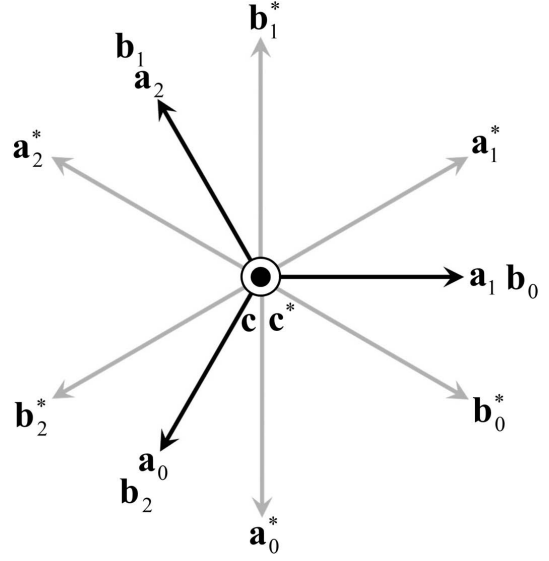


Figure C.3: Real (black) and reciprocal (gray) primitive translation vectors.

C.1.3 Derivation of extinction rule due to 3_1 screw axis

Similarly to the description in Appendix B §B.5 [p.31], the extinction due to 3_1 screw axis can be derived as follows.

Symmetry due to 3_1 screw axis at the origin is described as follows:

$$\begin{aligned}\rho[T_{3_1}^{(i)}(\mathbf{r})] &= \rho[T_{3_1}^{(0)}(\mathbf{r})], \quad i \in \{0, 1, 2\}. \\ T_{3_1}^{(0)}(\mathbf{r}) &= x\mathbf{a}_0 + y\mathbf{b}_0 + z\mathbf{c}, \\ T_{3_1}^{(1)}(\mathbf{r}) &= x\mathbf{a}_1 + y\mathbf{b}_1 + \left(\frac{1}{3} + z\right)\mathbf{c}, \\ T_{3_1}^{(2)}(\mathbf{r}) &= x\mathbf{a}_2 + y\mathbf{b}_2 + \left(\frac{2}{3} + z\right)\mathbf{c}.\end{aligned}\quad (\text{C.1})$$

On the other hand, referring to Fig. C.3, the following relations are evident.

$$\begin{aligned}\mathbf{a}_1 &= \mathbf{b}_0, \\ \mathbf{b}_1 &= -\mathbf{a}_0 - \mathbf{b}_0, \\ \mathbf{a}_2 &= -\mathbf{a}_0 - \mathbf{b}_0, \\ \mathbf{b}_2 &= \mathbf{a}_0,\end{aligned}$$

Substituting the above equation into (C.1),

$$\begin{aligned}\rho[T_{3_1}^{(i)}(\mathbf{r})] &= \rho[T_{3_1}^{(0)}(\mathbf{r})], \quad i \in \{0, 1, 2\}. \\ T_{3_1}^{(0)}(\mathbf{r}) &= x\mathbf{a}_0 + y\mathbf{b}_0 + z\mathbf{c}, \\ T_{3_1}^{(1)}(\mathbf{r}) &= -y\mathbf{a}_0 + (x - y)\mathbf{b}_0 + \left(\frac{1}{3} + z\right)\mathbf{c}, \\ T_{3_1}^{(2)}(\mathbf{r}) &= (-x + y)\mathbf{a}_0 - x\mathbf{b}_0 + \left(\frac{2}{3} + z\right)\mathbf{c}.\end{aligned}$$

The extinction condition can be described similarly to (B.2) [p.31] as follows:

$$\sum_{i=0}^2 \exp[-i2\pi \mathbf{h} \cdot T_{3_1}^{(i)}(\mathbf{r})] = 0. \quad (\text{C.2})$$

Here, for mathematical convenience to calculate \sum of (C.2), let us define $f_{3_1}(\mathbf{h}, \mathbf{r})$ as follows:

$$f_{3_1}(\mathbf{h}, \mathbf{r}) = \exp[-i2\pi(lz)].$$

Therefore, (C.2) can be deformed as follows:

$$\begin{aligned} & f_{3_1}(\mathbf{h}, \mathbf{r}) \times \\ & \left\{ \exp\{-i2\pi[hx + ky]\} \right. \\ & + \exp\{-i2\pi[-hy + k(x - y) + l\frac{1}{3}]\} \\ & \left. + \exp\{-i2\pi[+h(-x + y) - kx + l\frac{2}{3}]\} \right\} = 0. \end{aligned}$$

Since terms $[hx + ky]$, $[-hy + k(x - y)]$ and $[h(-x + y) - kx]$ in $\exp\{ \}$ of the above equation depend on value of x and y , the extinction can be discussed only when $h = k = l = 0$. Under this condition, the extinction condition can be described as follows:

$$1 + \exp(-i2\pi l \frac{1}{3}) + \exp(-i2\pi l \frac{2}{3}) = 0.$$

The second and third terms of on the left-hand side of the above equation are 1 and 1 not giving extinction when $l = 3n$, $\exp(-i2\pi \frac{1}{3})$ and $\exp(-i2\pi \frac{2}{3})$ giving extinction and $\exp(-i2\pi \frac{2}{3})$ and $\exp(-i2\pi \frac{1}{3})$ giving extinction. Therefore, the reflection condition can be described as follows:

$$000l : l = 3n.$$

With similar consideration, the same reflection condition for 3_2 can be derived.

C.1.4 On the absence of extinction due to 2_1 screw axis perpendicular to \mathbf{c} .

In Fig. C.1 [p.37], there are 2_1 screw axes perpendicular to \mathbf{c} at positions of $x = \frac{1}{2}$ and $y = \frac{1}{2}$. However, these 2_1 screw axes cause no extinction. The reason is that the angle spanned by \mathbf{a} and \mathbf{a}^* and that spanned by \mathbf{b} and \mathbf{b}^* are not zero (not parallel). About this, refer to the following description, please.

Symmetric operation due to rotation around \mathbf{a}_0 is represented by movement of point on a plane perpendicular to \mathbf{a}_0 . Referring to Fig. C.3, reciprocal vectors perpendicular to \mathbf{a}_0 are \mathbf{c}_0^* and \mathbf{b}_0^* . A real vector parallel to \mathbf{b}_0^* is represented by a linear combination of \mathbf{a}_0 and \mathbf{b}_0 , as $\frac{1}{2}\mathbf{a}_0 + \mathbf{b}_0$. Therefore, Symmetry due to 2_1 screw axis in the direction of \mathbf{a}_0 located at $(y, z) = \frac{1}{2}, \frac{1}{3}$ is represented as follows:

$$\begin{aligned} \rho[T_{2_1}^{(i)}(\mathbf{r})] &= \rho[T_{2_1}^{(0)}(\mathbf{r})], \quad i \in \{0, 1\}. \\ T_{2_1}^{(0)}(\mathbf{r}) &= x\mathbf{a}_0 \\ &+ (\frac{1}{2} + y)(\frac{1}{2}\mathbf{a}_0 + \mathbf{b}_0) \\ &+ (\frac{1}{3} + z)\mathbf{c} \\ &= (x + \frac{1}{4} + \frac{1}{2}y)\mathbf{a}_0 \\ &+ (\frac{1}{2} + y)\mathbf{b}_0 \\ &+ (\frac{1}{3} + z)\mathbf{c}, \\ T_{2_1}^{(1)}(\mathbf{r}) &= (\frac{1}{2} + x)\mathbf{a}_0 \\ &+ (\frac{1}{2} - y)(\frac{1}{2}\mathbf{a}_0 + \mathbf{b}_0) \\ &+ (\frac{1}{3} - z)\mathbf{c} \\ &= (x + \frac{3}{4} - \frac{1}{2}y)\mathbf{a}_0 \\ &+ (\frac{1}{2} - y)\mathbf{b}_0 \\ &+ (\frac{1}{3} - z)\mathbf{c}. \end{aligned}$$

The extinction condition (while not existing) is represented similarly to (B.2) [p.31] as follows:

$$\sum_{i=0}^1 \exp[-i2\pi \mathbf{h} \cdot T_{2_1}^{(i)}(\mathbf{r})] = 0. \quad (\text{C.3})$$

Here, for mathematical convenience to calculate \sum of (C.3), let us define $f_{2_1}(\mathbf{h}, \mathbf{r})$ as follows:

$$f_{2_1}(\mathbf{h}, \mathbf{r}) = \exp\{-i2\pi[h(\frac{1}{2} + x) + k\frac{1}{2} + l\frac{1}{3}]\}.$$

Therefore, \sum of (C.3) can be deformed as fol-

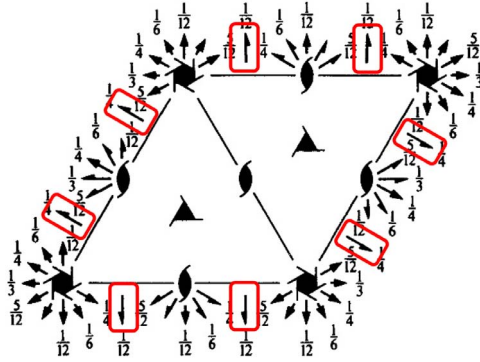


Figure C.4: *International Tables for Crystallography* (2006) Vol.A, Symmetric elements. $P6_122$ (#178).

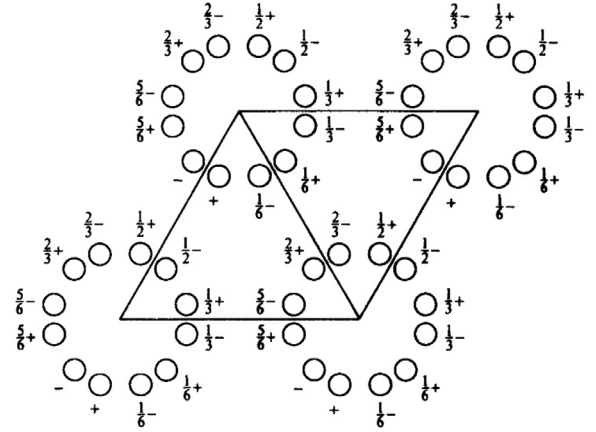


Figure C.5: *International Tables for Crystallography* (2006) Vol.A, Positions of atoms. $P6_122$ (#178).

lows:

$$\begin{aligned}
 & f_{2_1}(\mathbf{h}, \mathbf{r}) \times \\
 & \left\{ \exp\left\{-i2\pi\left[h\left(\frac{1}{4} - \frac{1}{2}y\right) - ky - lz\right]\right\} \right. \\
 & \left. + \exp\left\{-i2\pi\left[-h\left(\frac{1}{4} - \frac{1}{2}y\right) + ky + lz\right]\right\} \right\} \\
 & = f_{2_1}(\mathbf{h}, \mathbf{r}) \times \\
 & \cos\left\{2\pi\left[h\left(\frac{1}{4} - \frac{1}{2}y\right) - ky - lz\right]\right\} = 0.
 \end{aligned}$$

The above equation reveals that there is no extinction due to 2_1 screw axis perpendicular to \mathbf{c} since terms of h , k and l all depend to values of y or z . The second term $-h\frac{1}{2}y$ in $\cos\{\}$ of the above equation exists since \mathbf{a}_0 is not parallel to \mathbf{a}_0^* . If there were a reciprocal primitive vector parallel to the screw axis, we can discuss the extinction under the condition that $k, l = 0$. When there is no reciprocal primitive vector parallel to the screw axis, there is no extinction due to it.

In a similar way, it can be verified that there is no extinction due to screw axes parallel to \mathbf{b}_0 or $\mathbf{a}_0 + \mathbf{b}_0$.

C.2 Case of hexagonal system

C.2.1 Figure shown in *International Tables for Crystallography* (2006) Vol.A

Fig. C.4 is a drawing for space group $P6_122$ (#178) in *International Tables for Crystallography* (2006) Vol.A that shows symmetric elements. Fig. C.5 shows coordinates of atoms.

The unit cell is usually taken similarly to that in the case of trigonal system as shown in Fig. C.1 [p.37] and C.2 [p.37]. There are 2_1 screw axes perpendicular to \mathbf{c} . However they do not cause extinction similarly to the case of trigonal system.

C.2.2 Coordinates for describing six-fold screw axes

For describing positions of atoms that are rotated by $\frac{i}{6}2\pi$ ($i \in \{0, 1, 2, 3, 4, 5\}$) from the original position, let us prepare combinations of \mathbf{a}_i and \mathbf{b}_i as follows:

\mathbf{a}_i	\mathbf{b}_i	i
\mathbf{a}_0	\mathbf{b}_0	0
$\mathbf{a}_0 + \mathbf{b}_0$	$-\mathbf{a}_0$	1
\mathbf{b}_0	$-\mathbf{a}_0 - \mathbf{b}_0$	2
$-\mathbf{a}_0$	$-\mathbf{b}_0$	3
$-\mathbf{a}_0 - \mathbf{b}_0$	\mathbf{a}_0	4
$-\mathbf{b}_0$	$\mathbf{a}_0 + \mathbf{b}_0$	5

By using the above coordinates, positions that is rotated by $\frac{i}{6}2\pi$ ($i \in \{0, 1, 2, 3, 4, 5\}$) from the

original position can be written as follows:

$$\begin{aligned} x_0 &= x, & y_0 &= y, \\ x_1 &= x - y, & y_1 &= x, \\ x_2 &= -y, & y_2 &= x - y, \\ x_3 &= -x, & y_3 &= -y, \\ x_4 &= -x + y, & y_4 &= -x, \\ x_5 &= y, & y_5 &= -x + y. \end{aligned}$$

C.2.3 Derivation of extinction rule due to 6_1 screw axis

Symmetry due to 6_1 screw axis located at the origin in the direction of \mathbf{c} , is described as follows:

$$\begin{aligned} \rho[T_{6_1}^{(i)}(\mathbf{r})] &= \rho[T_{6_1}^{(0)}(\mathbf{r})], \quad i \in \{0, 1, 2, 3, 4, 5\}. \\ T_{6_1}^{(0)}(\mathbf{r}) &= x\mathbf{a}_0 + y\mathbf{b}_0 + z\mathbf{c}, \\ T_{6_1}^{(1)}(\mathbf{r}) &= (x - y)\mathbf{a}_0 + x\mathbf{b}_0 + \left(\frac{1}{6} + z\right)\mathbf{c}, \\ T_{6_1}^{(2)}(\mathbf{r}) &= -y\mathbf{a}_0 + (x - y)\mathbf{b}_0 + \left(\frac{2}{6} + z\right)\mathbf{c}, \\ T_{6_1}^{(3)}(\mathbf{r}) &= -x\mathbf{a}_0 - y\mathbf{b}_0 + \left(\frac{3}{6} + z\right)\mathbf{c}, \\ T_{6_1}^{(4)}(\mathbf{r}) &= (-x + y)\mathbf{a}_0 - x\mathbf{b}_0 + \left(\frac{4}{6} + z\right)\mathbf{c}, \\ T_{6_1}^{(5)}(\mathbf{r}) &= y\mathbf{a}_0 + (-x + y)\mathbf{b}_0 + \left(\frac{5}{6} + z\right)\mathbf{c}. \end{aligned}$$

Similarly to (B.2) [p.31], the extinction condition is described as follows:

$$\sum_{i=0}^5 \exp[-i2\pi\mathbf{h} \cdot T_{6_1}^{(i)}(\mathbf{r})] = 0. \quad (\text{C.4})$$

For mathematical convenience, let us define $f_{6_1}(\mathbf{h}, \mathbf{r})$ as follows:

$$f_{6_1}(\mathbf{h}, \mathbf{r}) = \exp[-i2\pi(lz)].$$

From (C.4), the extinction condition is obtained as follows:

$$\begin{aligned} f_{6_1}(\mathbf{h}, \mathbf{r}) \times \\ \left\{ \exp\{-i2\pi[hx + ky]\} \right. \\ + \exp\{-i2\pi[h(x - y) + kx + l\frac{1}{6}]\} \\ + \exp\{-i2\pi[-hy + k(x - y) + l\frac{2}{6}]\} \\ + \exp\{-i2\pi[-hx - ky + l\frac{3}{6}]\} \\ + \exp\{-i2\pi[h(-x + y) - kx + l\frac{4}{6}]\} \\ \left. + \exp\{-i2\pi[hy + k(-x + y) + l\frac{5}{6}]\} \right\} = 0. \end{aligned}$$

The extinction can be discussed only when $h = k = i = 0$. Under this condition, the above extinction condition can be described as follows:

$$\begin{aligned} 1 \\ + \exp(-i2\pi l \frac{1}{6}) \\ + \exp(-i2\pi l \frac{2}{6}) \\ + \exp(-i2\pi l \frac{3}{6}) \\ + \exp(-i2\pi l \frac{4}{6}) \\ + \exp(-i2\pi l \frac{5}{6}) = 0. \quad (\text{C.5}) \end{aligned}$$

When $l = 6n$, reflections do not distinguish. When $l = 6n + i$ ($i \in \{1, 2, 3, 4, 5\}$), reflections distinguish since phase interval of the six term is an identical value $-2\pi\frac{i}{6}$. The reflection condition (not extinct) can be described as follows,

$$hkil : l = 6n.$$

Similarly, the same reflection condition can be derived also for 6_1 screw axis.

In Fig. C.4, 2_1 and 3_1 screw axes in the direction of \mathbf{c} are found. However, the logical product of reflection conditions due to 6_1 , 2_1 and 3_1 screw axes gives the same reflection condition as described in the above equation.

C.2.4 Derivation of the extinction due to 6_2 screw axis

The extinction condition due to 6_2 screw axis is given similarly to (C.5) [p.41] as follows:

$$\begin{aligned}
 & 1 \\
 & + \exp(-i2\pi l \frac{1}{3}) \\
 & + \exp(-i2\pi l \frac{2}{3}) \\
 & + 1 \\
 & + \exp(-i2\pi l \frac{1}{3}) \\
 & + \exp(-i2\pi l \frac{2}{3}) = 0.
 \end{aligned}$$

When $l = 3n$, reflections do not distinguish since the six term have an identical value unity. When $l = 3n + i$ ($i \in \{1, 2\}$), reflections distinguish since phase interval of the six term is an identical value $-2\pi \frac{i}{3}$. Then, the reflection condition (not extinct) is given by

$$hkl : l = 3n.$$

In a similar way, the same reflection condition

can be derived for 6_4 screw axis.

C.2.5 Derivation of extinction rule due to 6_3 screw axis

An equation for 6_3 screw axis that corresponds to (C.5) [p.41] is given by

$$\begin{aligned}
 & 1 \\
 & + \exp(-i2\pi l \frac{1}{2}) \\
 & + 1 \\
 & + \exp(-i2\pi l \frac{1}{2}) \\
 & + 1 \\
 & + \exp(-i2\pi l \frac{1}{2}) = 0.
 \end{aligned}$$

When l is even, all terms are unity giving no extinction. When l is odd, reflections distinguish since phase interval of the six terms is an identical value $-2\pi \frac{1}{2}$ giving extinction. Therefore, the reflection condition (not extinct) is given by

$$hkl : l = 2n.$$

End of the document.

Index

Symbols

2_1 screw axis	27, 30
<i>A</i> base-centered lattice	30
<i>B</i> base-centered lattice	30
<i>C</i> base-centered lattice	30
<i>c</i> glide plane	27, 30
<i>n</i> glide plane	30
‘Face-centered monoclinic’	25

A

<i>Aba2</i> (#41)	28
<i>Abm2</i> (#39)	28
Absolute structure	6, 15
Absorption correction	6
Account	1
Acta Cryst. C	15
Administrator	1
Administration	1
ALART	15
All hydrogens buttons	12
<i>Ama2</i> (#40)	28
<i>Amm2</i> (#38)	28
Anisotropic temperature factor	9, 10
Anomalous dispersion	6
Auto button	i, 7
Average	6

B

Ball and stick	16
Base-centered lattice	30, 31
Body-centered lattice	32
Body-centered monoclinic lattice	26
Bragg reflection plane	22
Bragg’s reflection condition	20, 22, 26
Bravais lattice	25, 26

C

<i>C12/c1</i>	29, 30
<i>C2/c</i> (#15)	29, 30
Cell choice	27
Centrosymmetric crystal	7
CIF	15
Cif.Cif	16
Cif.cif	17

Complex lattice	26, 27, 31
Crystal system	26
CrystalClear.cif	16
Crystals	4, 8
CRYSTALS Server	2
Crystl system	27
Cubic	25

D

D amino acid	29, 33
Default	9
Dell computer	i
Determination of space group	24, 25
Direct method	7
Display menu	16
Drawing of Miller	23
Dynamical diffraction	14

E

Equivalent diffraction	6, 7
Equivalent reflection	6, 7
Ewald, P. P.	20–22
Ewald construction	20–22
Ewald sphere	20, 22
Ewald’s reflection condition	22
Extinction effect	14
Extinction rule	20, 24, 25, 27, 32

F

F	13
F-squared	13
Face-centered lattice	32
Flack parameter	6, 14
Friedel mates	6
Friedel’s law	6

G

Glide plane	30–32
Graphic symbol of 2_1 screw axis	27
Graphic symbol of <i>c</i> glide plane	27
Graphic symbol of symmetric center	27

H

H-M full notation	27, 28, 30
-------------------	------------

H-M notation	27–29	$P112_1/n$	28
Hard	9	$P12_1/a$	28
Hauptman, H. A.	7	$P12_1/c$	28
Hermann-Mouguin full notation	27, 28	$P12_1/n1$	28
Hermann-Mouguin notation	27–29	$P12_11$	29, 30
Hexagonal	25	$P2_1(\#4)$	29, 30
Horizontal translation	i	$P2_1/b11$	28
Hydroxy radio button	11	$P2_1/c(\#14)$	24–26, 28, 29
Hydroxyl oxygen	12	$P2_1/c(\#14)$	25
		$P2_1/c11$	28
		$P2_1/n11$	28
I			
Image due to 2_1 screw axis	27	$P2_111$	30
Image due to c glide plane	27	$P2_12_12_1(\#19)$	29, 30
In-plane rotation	i	$P3_121(\#152)$	37
Initial phases	7, 9	$P6_122(\#178)$	39–41
Invert structure	15	$P\bar{1}(\#2)$	29, 30
Isotropic temperature factor	10	Password	i, 1
Isotropic temperature factors	9	Phase determination	7, 9
		Phase problem	7, 27, 29
K			
Karle, J.	7	Position of atom	27
		Primitive lattice	26
		Primitive translation vector	21
		process.out	6, 25
L			
L amino acid	29, 33		
Laue, M. T. F. von	20, 21		
Laue group	25–27		
Laue's reflection condition	20–22		
Least squares button	13		
Login name	i, 1, 3		
M			
Max. Shift / Error	15		
Methine carbon	11, 12		
Methylene carbon	11, 12		
Miller indices	23		
molecular formula	4		
Monoclinic	26, 29		
Monoclinic	25, 26, 28, 30		
N			
Nishikawa, S.	26		
None radio button	11		
O			
Open project	3		
Optical isomer	33		
Ordinal number of space group	27		
Orthorhombic	25, 30		
P			
$P112_1$	30		
$P112_1/a$	28		
$P112_1/b$	28		
S			
Schönflies notation	27		
Screw axis	27, 30, 31, 34, 35, 37		
Send CIF	17		
Set of the diffractometer	4		
Sheldrick	13		
Shelx	4, 8		
Shelxl	9		
Shelxl2013	9		
Sigma cutoff:	13		
SIR	9		
SIR92	7, 9		
Six-fold screw axis	37		

INDEX

45

Space group	24–27	Unique axis	27
Style submenu	16	Users	2
Sucrose	i	Utility menu	15
Symmetric center	27, 30	V	
Symmetric element	26	Vertical translation	i
Symmetry	20		
T		W	
Taurine	24–26	Weighted average	6
Tetragonal	25	Weights:	13
Thermal ellipsoid	17, 18	Wyckoff, R. W. G.	26
Three-fold screw axis	37	X	
Tools	1	X-ray setting	4
Triclinic	25, 30	Z	
Trigonal	25	Z value	4
U		Zoom	i